1

Fundamental Optical Properties of Materials I

S.O. Kasap[1], *W.C. Tan*[2], *Jai Singh*[3], *and Asim K. Ray*[4]

[1] *Department of Electrical and Computer Engineering, University of Saskatchewan, 57 Campus Drive, Saskatoon, Canada*
[2] *Department of Electrical & Computer Engineering, National University of Singapore, Kent Ridge, Singapore*
[3] *College of Engineering, IT and Environment, Purple 12, Charles Darwin University, Ellengowan Drive, Darwin, Australia*
[4] *Department of Electrical & Computer Engineering, Brunel University London, Kingston Lane, Uxbridge, UK*

CHAPTER MENU

1.1 Introduction

Optical properties of a material change or affect the characteristics of light passing through it by modifying its propagation vector or intensity. Two of the most important optical parameters are the refractive index n and the extinction coefficient K, which are generically called *optical constants*, although some authors include other optical coefficients within this terminology. The latter is related to the attenuation or absorption coefficient α. In Part I, in this chapter, we present the complex refractive index, the frequency or wavelength dependence of n and K, so-called dispersion relations, how n and K are inter-related, and how n and K can be determined by studying the transmission as a function of wavelength through a thin film of the material. Physical insights into n and K are provided in Part II (Chapter 2). In addition, there has been a strong research interest in characterizing the optical properties of inhomogeneous media, such as porous media, in which both light absorption and scattering take place so that the reflectance is not specular but diffuse. The latter problem is now included in this second edition.

The optical properties of various materials, with n and K being the most important, are available in the literature in one form or another, either published in journals, books, and handbooks, or posted on websites of various researchers, organizations (e.g. NIST), or companies (e.g. Schott Glass). Nonetheless, the reader is referred to the

Optical Properties of Materials and Their Applications, Second Edition. Edited by Jai Singh.

works of Greenway and Harbeke [1], Wolfe [2], Klocek [3], Palik [4, 5], Ward [6], Efimov [7], Palik and Ghosh [8], Nikogosyan [9], and Weaver and Frederikse [10] for the optical properties of a wide range of materials. Adachi's books on the optical constants of semiconductors are highly recommended [11–13], along with Madelung's third edition of *Semiconductors: Data Handbook* [14]. There are, of course, other books and handbooks that also contain optical constants in various chapters; see, for example, references [15–20]. There are also various books that describe optical properties of solids at the senior undergraduate and introductory graduate levels, such as those by Tanner [21], Jimenez and Tomm [22], Stenzel [23], Fox [24], Simmons and Potter [25], Toyozawa [26], Wooten [27], and Abeles [28], which are highly recommended.

A number of experimental techniques are available for measuring n and K, some of which have been summarized by Simmons and Potter [25]. For example, ellipsometry measures changes in the polarization of light incident on a sample to sensitively characterize surfaces and thin films (see Chapter 23 in this volume). The interaction of incident polarized light with the sample causes a polarization change in the light, which may then be measured by analyzing the light reflected from the sample. Collins has also provided an extensive in-depth review of ellipsometry for optical measurements [29]. One of the most popular and convenient optical experiments involves a monochromatic light passing through a thin sample, and measuring the transmitted intensity as a function of wavelength, $T(\lambda)$, using a simple spectrophotometer. For thin samples on a thick transparent substrate, the transmission spectrum shows oscillations in $T(\lambda)$ with the wavelength due to interferences within the thin film. Swanepoel's technique uses the $T(\lambda)$ measurement to determine n and K, as described in Section 1.4.

1.2 Optical Constants *n* and *K*

One of the most important optical constants of a material is its refractive index, which in general depends on the wavelength of the electromagnetic (EM) wave, through a relationship called *dispersion*. In materials where an EM wave loses its energy during its propagation, the refractive index becomes complex. The real part is usually the refractive index, n, and the imaginary part is called the *extinction coefficient*, K. In this section, the refractive index and extinction coefficient will be presented in detail, along with some common dispersion relations. A more practical and a semiquantitative approach is taken along the lines in [30] rather than a full dedication to rigor and mathematical derivations. More analytical approaches can be found in other texts, such as [25, 26].

1.2.1 Refractive Index and Extinction Coefficient

The refractive index of an optical or dielectric medium, n, is the ratio of the velocity of light c in vacuum to its velocity v in the medium; $n = c/v$. Using this and Maxwell's equations, one obtains the well-known Maxwell's formula for the refractive index of a substance as $n = \sqrt{\varepsilon_r \mu_r}$, where ε_r is the static dielectric constant or relative permittivity and μ_r the relative magnetic permeability of the medium. As $\mu_r = 1$ for nonmagnetic substances, one gets $n = \sqrt{\varepsilon_r}$, which is very useful in relating the dielectric properties to optical properties of materials at any particular frequency of interest. As ε_r depends on the wavelength of light, the refractive index also depends on the wavelength of light, and

this dependence is called *dispersion*. In addition to dispersion, an EM wave propagating through a lossy medium experiences attenuation, which means it loses its energy, due to various loss mechanisms such as the generation of phonons (lattice waves), photogeneration, free carrier absorption, scattering, etc. In such materials, the refractive index becomes a complex function of the frequency of the light wave. The complex refractive index in this chapter is denoted by n^*, with real part n, and imaginary part K, called the *extinction coefficient*, is related to the complex relative permittivity, $\varepsilon_r = \varepsilon_r' + i\varepsilon_r''$, by,

$$n^* = n + iK = \sqrt{\varepsilon_r} = \sqrt{\varepsilon_r' + i\varepsilon_r''} \tag{1.1a}$$

where ε_r' and ε_r'' are, respectively, the real and imaginary parts of ε_r. Eq. (1.1a) gives:

$$n^2 - K^2 = \varepsilon_r' \text{ and } 2nK = \varepsilon_r''. \tag{1.1b}$$

In explicit terms, n and K can be obtained as

$$n = (1/\sqrt{2})[(\varepsilon_r'^2 + \varepsilon_r''^2)^{1/2} + \varepsilon_r']^{1/2} \tag{1.2a}$$

$$K = (1/\sqrt{2})[(\varepsilon_r'^2 + \varepsilon_r''^2)^{1/2} - \varepsilon_r']^{1/2} \tag{1.2b}$$

Some books (particularly in electrical engineering) use $\varepsilon_r = \varepsilon_r' - i\varepsilon_r''$ and $n^* = n - iK$ instead of $\varepsilon_r = \varepsilon_r' + i\varepsilon_r''$ and $n^* = n + iK$. The preference lies in what was assumed for the propagating electric field, whether it is represented by $\exp i(\omega t - kx)$ or $\exp i(kx - \omega t)$, where k is the propagation constant. In a lossy medium, the imaginary part of n^* must lead to a traveling wave whose amplitude decays. Notice that, for $\varepsilon_r'' \ll \varepsilon_r'$, $n = \sqrt{\varepsilon_r'}$ and $K = \varepsilon_r''/2n$—that is, the refractive index is essentially determined by the real part of ε_r and K is determined by the imaginary part of ε_r, which is known to represent losses in a dielectric medium.

The extinction coefficient K represents loss from the energy carried by the propagating EM wave by conveniently including this loss as the imaginary part in the complex refractive index. The optical attenuation coefficient α gauges the rate of this loss from the propagating EM wave. In the absence of scattering, the attenuation would be due to absorption within the medium. For an EM wave that is propagating along x with an intensity I, α is defined by

$$\alpha = -\frac{dI}{Idx} \tag{1.3}$$

We can relate α and K quite easily by taking a plane wave traveling along x for which the electric field in the wave propagates as $E = E_o \exp i(kx - \omega t)$, where E_o is a constant, ω is the angular frequency and k is the complex propagation constant in the medium, related to n^* by its definition $k = n^*\omega/c = (n + iK)(\omega/c)$. In free space $k = k_o = \omega/c = 2\pi/\lambda$, where λ is the free space wavelength. We can substitute for n^* and then use I is proportional to $|E|^2$ to find $I \propto \exp[-2(\omega/c)Kx)]$—that is, I decays exponentially with the distance propagated. We can substitute for I in (1.3) to find

$$\alpha = \frac{2\omega}{c}K \tag{1.4}$$

The optical constants n and K can be determined by measuring the reflectance from the surface of a material as a function of polarization and the angle of incidence. For normal incidence, the reflection coefficient, r, is obtained as

$$r = \frac{1 - n^*}{1 + n^*} = \frac{1 - n - iK}{1 + n + iK} \tag{1.5}$$

The reflectance R is then defined by:

$$R = |r|^2 = \left|\frac{1 - n - iK}{1 + n + iK}\right|^2 = \frac{(1-n)^2 + K^2}{(1+n)^2 + K^2}. \tag{1.6}$$

Notice that whenever K is large, for example, over a range of wavelengths, the absorption is strong, and the reflectance is almost unity. The light is then reflected, and any light in the medium is highly attenuated (typical sample calculations may be found in [24, 30]).

Optical properties of materials are typically presented either by showing the frequency dependences (dispersion relations) of n and K or ε_r' and ε_r''. An intuitive guide to explaining dispersion in insulators is based on a single oscillator model in which the electric field in the light induces forced dipole oscillations in the material (displaces the electron shells in an atom to oscillate about the positive nucleus) with a single resonant frequency ω_o. The frequency dependences of ε_r' and ε_r'' are then obtained as:

$$\varepsilon_r' = 1 + \frac{N_{\text{at}}}{\varepsilon_o}\alpha_e' \text{ and } \varepsilon_r'' = 1 + \frac{N_{\text{at}}}{\varepsilon_o}\alpha_e'', \tag{1.7}$$

where N_{at} is the number of atoms per unit volume, ε_o is the vacuum permittivity, and α_e' and α_e'' are, respectively, the real and imaginary parts of the electronic polarizability, given respectively by:

$$\alpha_e' = \alpha_{eo}\frac{1 - (\omega/\omega_o)^2}{[1 - (\omega/\omega_o)^2]^2 + (\gamma/\omega_o)^2(\omega/\omega_o)^2} \tag{1.8a}$$

and

$$\alpha_e'' = \alpha_{eo}\frac{(\gamma/\omega_o)(\omega/\omega_o)}{[1 - (\omega/\omega_o)^2]^2 + (\gamma/\omega_o)^2(\omega/\omega_o)^2} \tag{1.8b}$$

where α_{eo} is the DC polarizability corresponding to $\omega = 0$ and γ is the loss coefficient that characterizes the EM wave losses within the material system. Using Eqs. (1.1)–(1.2) and (1.7)–(1.8), the frequency dependence of n and K can be studied. Figure 1.1a shows the dependence of n and K on the normalized frequency ω/ω_o for a simple single electronic dipole oscillator of resonance frequency ω_o.

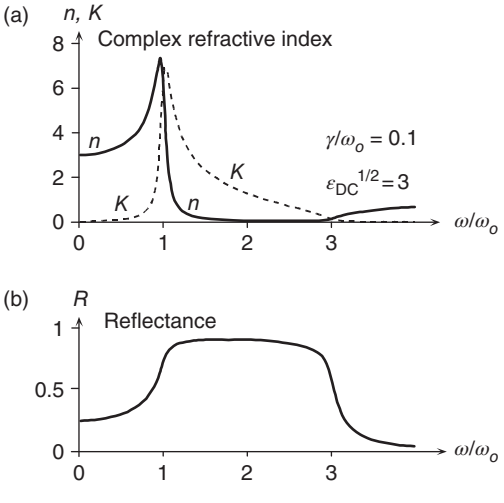

Figure 1.1 Refractive index n and extinction coefficient K obtained from a single electronic dipole oscillator model. (a) n and K versus normalized frequency, and (b) reflectance versus normalized frequency.

It is seen from Figure 1.1 that n and K peak close to $\omega = \omega_o$. If a material has a $\varepsilon_r'' \gg \varepsilon_r'$, then $\varepsilon_r \approx i\varepsilon_r''$, and $n \approx K \approx \sqrt{\varepsilon_r''/2}$ is obtained from Eq. (1.1b). Figure 1.1b shows the dependence of the reflectance R on the frequency. It is observed that R reaches its maximum value at a frequency slightly above $\omega = \omega_o$, and then remains high until ω reaches nearly $3\omega_o$; thus, the reflectance is substantial while absorption is strong. The normal dispersion region is the frequency range below ω_o, where n falls as the frequency decreases; that is, n decreases as the wavelength λ increases. Anomalous dispersion region is the frequency range above ω_o where n decreases as ω increases. Below ω_o, K is small and, if ε_{DC} is ε_r (0), the DC permittivity, then

$$n^2 \approx 1 + (\varepsilon_{DC} - 1)\frac{\omega_o^2}{\omega_o^2 - \omega^2}; \omega < \omega_o. \tag{1.9}$$

Since, $\lambda = 2\pi c/\omega$, defining $\lambda_o = 2\pi c/\omega_o$ as the resonance wavelength, one gets:

$$n^2 \approx 1 + (\varepsilon_{DC} - 1)\frac{\lambda^2}{\lambda^2 - \lambda_o^2}; \lambda > \lambda_o. \tag{1.10}$$

While intuitively useful, the dispersion relations in Eq. (1.8) are far too simple. More rigorously, we have to consider the dipole oscillator quantum mechanically, which means a photon excites the oscillator to a higher energy level—see, for example, Fox [24] or Simmons and Potter [25]. The result is that we would have a series of $\lambda^2/(\lambda^2 - \lambda_i{}^2)$ terms with various weighting factors A_i that add to unity, where λ_i represent different resonance wavelengths. The weighting factors A_i involve quantum mechanical matrix elements.

Figure 1.2 shows the complex relative permittivity and the complex refractive index of crystalline silicon in terms of photon energy $h\nu$ [31, 32]. For photon energies below the bandgap energy (1.1 eV), both ε_r'' and K are negligible and n is close to 3.7. Both ε_r'' and K increase and change strongly as the photon energy becomes greater than 3 eV, far beyond the bandgap energy. Notice that both ε_r'' and K peak at $h\nu \approx 3.5$ eV, which corresponds to a direct photoexcitation processes, electrons excited directly from the valence band to the conduction band, as discussed in Chapter 2.

1.2.2 *n* and *K*, and Kramers–Kronig Relations

If we know the frequency dependence of the real part, ε_r', of the relative permittivity of a material, we can, using the *Kramers–Kronig relations* between the real and the imaginary parts, determine the frequency dependence of the imaginary part ε_r'', and vice versa. The transform requires that we know the frequency dependence of either the real or imaginary part over as wide a range of frequencies as possible, ideally from zero (DC) to infinity, and that the material has linear behavior, that is, it has a relative permittivity that is independent of the applied field. The Kramers–Kronig relations for the relative permittivity $\varepsilon_r = \varepsilon_r' + i\varepsilon_r''$ are given by [33–35] (see also Appendix 1C in [25] as well as [27])

$$\varepsilon_r'(\omega) = 1 + \frac{2}{\pi}P\int_0^\infty \frac{\omega'\varepsilon''_r(\omega')}{\omega'^2 - \omega^2}d\omega' \tag{1.11a}$$

and

$$\varepsilon_r''(\omega) = -\frac{2\omega}{\pi}P\int_0^\infty \frac{\varepsilon_r'(\omega') - 1}{\omega'^2 - \omega^2}d\omega' \tag{1.11b}$$

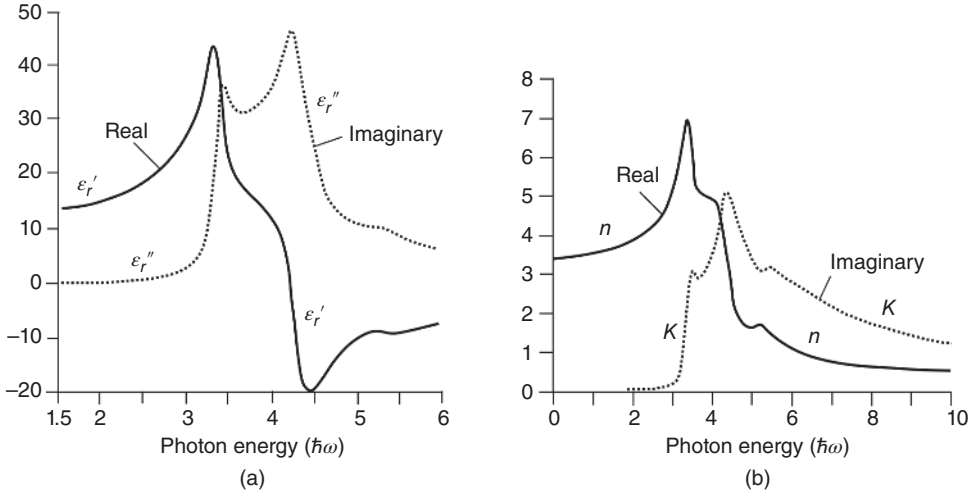

Figure 1.2 (a) Complex relative permittivity of a silicon crystal as a function of photon energy plotted in terms of real (ε_r') and imaginary (ε_r'') parts. (b) Optical properties of a silicon crystal vs. photon energy in terms of real (n) and imaginary (K) parts of the complex refractive index. Source: Adapted from D. E. Aspnes and A. A. Studna, 1983 [32] and H.R. Philipp and E.A. Taft, 1960 [31].

where ω' is the integration variable, P represents the Cauchy principal value of the integral, and the singularity at $\omega = \omega'$ is avoided.

Similarly, one can relate the real and imaginary parts of the polarizability, $\alpha'(\omega)$ and $\alpha''(\omega)$, and those of the complex refractive index, $n(\omega)$ and $K(\omega)$, as well. For a complex refractive index written as $n^* = n(\omega) + iK(\omega)$,

$$n(\omega) = 1 + \frac{2}{\pi} P \int_0^\infty \frac{\omega' K(\omega')}{\omega'^2 - \omega^2} d\omega' \text{ and } K(\omega) = -\frac{2}{\pi} P \int_0^\infty \frac{n(\omega') - 1}{\omega'^2 - \omega^2} d\omega' \qquad (1.12)$$

Although it appears, in theory, that one needs to integrate the spectrum of n or K from DC to infinite frequencies, this is obviously not feasible, and is unnecessary. It should be noted that the experimental setup usually has low- and high-frequency limitations that truncate the preceding integrations. Moreover, in many cases, we are interested in the spectrum of n and K in and around an absorption band. Thus, before and after the absorption frequency range, K would be negligibly small, and we can use this absorption frequency range in the preceding integrals in Eq. (1.12). There are numerous studies in the literature that use the preceding Kramers–Kronig relations in extracting the wavelength dependence of n from that of K, and vice versa, especially around clear absorption bands; a few selected examples can be found in [36–40], and there are many others in the literature. There are also several useful approaches in which the absorption spectrum, or $K(\omega)$, is described in terms of a particular physical model with a particular expression, and the corresponding refractive index $n(\omega)$ is derived from the Kramers–Kronig transformation for both amorphous and crystalline solids—for examples, see [41, 42].

It should be emphasized that the optical constants n and K have to obey what are called *f-sum rules* [43]. For example, the integration of $[n(\omega) - 1]$ over all frequencies must be zero, and the integration of $\omega K(\omega)$ over all frequencies gives $(\pi/2)\omega_p{}^2$, where $\omega_p = \hbar(4\pi NZe^2/m_e)^{1/2}$ is the free electron plasma frequency in which N is the atomic

concentration, Z is the total number of electrons per atom, and e and m_e are the charge and mass of the electron, respectively. The f-sum rules provide a consistency check and enable various constants to be interrelated.

1.3 Refractive Index and Dispersion

There are several popular models describing the spectral dependence of refractive index n in a material. Most of these are described in the following text, although some, such as the infrared refractive index, is covered in the discussion on Reststrahlen absorption in Part II, since it is closely related to the coupling of the EM wave to lattice vibrations. The most popular dispersion relation in optical materials is probably the Sellmeier relationship, since one can sum any number of resonance-type terms to get as wide a range of wavelength dependence as possible. However, its main drawback is that it does not accurately represent the refractive index when there is a contribution arising from free carriers in narrow bandgap or doped semiconductors.

There are many handbooks, books, and websites that now provide empirical equations for the refractive index of a wide range of solids, for example as in references [1–19, 44].

1.3.1 Cauchy Dispersion Relation

In the Cauchy relationship, the dispersion relationship between the refractive index (n) and the wavelength of light (λ) is commonly stated in the following form:

$$n = A + \frac{B}{\lambda^2} + \frac{C}{\lambda^4} \tag{1.13}$$

where A, B, and C are material-dependent specific constants. Equation (1.13) is known as *Cauchy's formula*; it is typically used in the visible spectrum region for various optical glasses, and it applies to *normal dispersion*, when n decreases with increasing λ [45, 46]. The third term is sometimes dropped for a simpler representation of n versus λ behavior. The original expression was a series in terms of the wavelength, λ, or frequency, ω, or photon energy $\hbar\omega$ of light as:

$$n = a_0 + a_2\lambda^{-2} + a_4\lambda^{-4} + a_6\lambda^{-6} + \ldots \lambda > \lambda_{\text{th}}, \tag{1.14a}$$

or

$$n = n_0 + n_2(\hbar\omega)^2 + n_4(\hbar\omega)^4 + n_6(\hbar\omega)^6 + \ldots \hbar\omega < \hbar\omega_{\text{th}}, \tag{1.14b}$$

where $\hbar\omega$ is the photon energy; $\hbar\omega_{\text{th}} = hc/\lambda_{\text{th}}$ is the optical excitation threshold (e.g. bandgap energy); and a_0, a_2,… and n_0, n_2,… are constants. It has been found that a Cauchy relation in the following form [47]:

$$n = n_{-2}(\hbar\omega)^{-2} + n_0 + n_2(\hbar\omega)^2 + n_4(\hbar\omega)^4, \tag{1.15}$$

can be used satisfactorily over a wide range of photon energies. The dispersion parameters of Eq. (1.15) are listed in Table 1.1 for a few selected materials over specific photon energy ranges.

Cauchy's dispersion relations given in Eqs. (1.13)–(1.14) were originally called the *elastic ether theory of the refractive index*. It has been widely used for many materials,

Table 1.1 Cauchy's dispersion parameters of Eq. (1.15) for Ge, Si, and Diamond from [43].

Material	$\hbar\omega$(eV) Min	$\hbar\omega$(eV) Max	n_{-2} (eV^2)	n_0	n_2 (eV^{-2})	n_4 (eV^{-4})
Diamond	0.0500	5.4700	-1.07×10^{-5}	2.378	0.00801	0.000104
Si	0.0020	1.08	-2.04×10^{-8}	3.4189	0.0815	0.0125
Ge	0.0020	0.75	-1.00×10^{-8}	4.0030	0.220	0.140

although, in recent years, many researchers have preferred to use the Sellmeier equation, described in the following text.

1.3.2 Sellmeier Equation

The Sellmeier equation [48] is an empirical relation between the refractive index n of a substance and wavelength λ of light in the form of a series of single dipole oscillator terms, each of which has the usual $\lambda^2/(\lambda^2-\lambda_i{}^2)$ dependence as in

$$n^2 = 1 + \frac{A_1\lambda^2}{\lambda^2-\lambda_1^2} + \frac{A_2\lambda^2}{\lambda^2-\lambda_2^2} + \frac{A_3\lambda^2}{\lambda^2-\lambda_3^2} \tag{1.16}$$

where A_1, A_2, A_3 and λ_1, λ_2, and λ_3 are constants, called *Sellmeier coefficients*, which are determined by fitting this expression to the experimental data. The actual Sellmeier formula is more complicated. It has more terms of similar form, such as $A_i\,\lambda^2/(\lambda^2-\lambda_i{}^2)$, where $i = 4, 5, \ldots$, but these can generally be neglected in representing n vs. λ behavior over typical wavelengths of interest and by ensuring that the three terms included in Eq. (1.16) correspond to the most important or relevant terms in the summation [49]. The Sellmeier coefficients for some materials, including pure Silica (SiO_2) and 86.5 mol% SiO_2–13.5 mol% GeO_2, are given in Table 1.2 as examples. A quantitative analysis of the application of the Sellmeier dispersion relation to a range of materials, from glasses to semiconductors, has been discussed by Tatian [49].

There are two methods for determining the refractive index of silica–germania glass $(SiO_2)_{1-x}(GeO_2)_x$. The first is a simple, but approximate, linear interpolation of the refractive index between known compositions, for example, $n(x) - n(0.135) = (x - 0.235)[n(0.135) - n(0)]/0.135$, where $n(x)$ is for $(SiO_2)_{1-x}(GeO_2)_x$; $n(0.135)$ is for 86.5 mol% SiO_2–13.5 mol% GeO_2; and $n(0)$ is for SiO_2. The second is an interpolation for coefficients A_i and λ_i between SiO_2 and GeO_2 as [50]:

$$n^2 - 1 = \frac{\{A_1(S) + X[A_1(G) - A_1(S)]\}\lambda^2}{\lambda^2 - \{\lambda_1(S) + X[\lambda_1(G) - \lambda_1(S)]\}\lambda_1^2} + \ldots, \tag{1.17}$$

where S and G in parentheses refer to silica and germania, respectively. The theoretical basis of the Sellmeier equation lies in representing the solid as a sum of N lossless (frictionless) Lorentz oscillators such that each has the usual form of $\lambda^2/(\lambda^2-\lambda_i{}^2)$ with different λ_i and each has a different strength, or weighting factor; A_i, $i = 1$ to N [51, 52]. Such dispersion relationships are essential in designing photonic devices such as waveguides. (Note that although A_i weighs different Lorentz contributions, they do not sum to 1 since they include other parameters besides the oscillator strength f_i.) The refractive indices of most optical glasses have been extensively modeled by the Sellmeier equation.

Table 1.2 Sellmeier coefficients of a few materials, where λ_1, λ_2, λ_3 are in μm.

Material	A_1	A_2	A_3	λ_1	λ_2	λ_3
SiO_2 (fused silica)	0.696749	0.408218	0.890815	0.0690660	0.115662	9.900559
86.5% SiO_2–13.5% GeO_2	0.711040	0.451885	0.704048	0.0642700	0.129408	9.425478
GeO_2	0.80686642	0.71815848	0.85416831	0.068972606	0.15396605	11.841931
Barium fluoride	0.3356	0.506762	3.8261	0.057789	0.109681	46.38642
Sapphire	1.023798	1.058264	5.280792	0.0614482	0.110700	17.92656
Diamond	0.3306	4.3356		0.175	0.106	
Quartz, n_o	1.35400	0.010	0.9994	0.092612	10.700	9.8500
Quartz, n_e	1.38100	0.0100	0.9992	0.093505	11.310	9.5280
KTP, n_o	1.2540	0.0100	0.0992	0.09646	6.9777	5.9848
KTP, n_e	1.13000	0.0001	0.9999	0.09351	7.6710	12.170

Source: From various sources.

Various optical glass manufacturers such as Schott Glass normally provide the Sellmeier coefficients for their glasses [53]. The optical dispersion relations for glasses have been discussed by a number of authors [7, 25, 54].

There are other Sellmeier–Cauchy-like dispersion relationships that inherently take account of various contributions to the optical properties, such as the electronic and ionic polarization and the interaction of photons with free electrons. For example, for many semiconductors and ionic crystals, two useful dispersion relations are,

$$n^2 = A + \frac{B\lambda^2}{\lambda^2 - C} + \frac{D\lambda^2}{\lambda^2 - E}, \tag{1.18}$$

and

$$n^2 = A + \frac{B}{\lambda^2 - \lambda_o^2} + \frac{C}{(\lambda^2 - \lambda_o^2)^2} + D\lambda^2 + E\lambda^4, \tag{1.19}$$

where A, B, C, D, E, and λ_o are constants particular to a given material. Eq. (1.18) is equivalent to the Sellmeier equation. Eq. (1.19) is known as the *Herzberger dispersion relation* [52]. Table 1.3 provides a few examples. Both Cauchy and Sellmeier equations are strictly applicable in wavelength regions where the material is transparent, that is, the extinction coefficient is relatively small. The refractive index dispersion relations

Table 1.3 Parameters of Eq. (1.19) for some selected materials.

Material	λ_o (μm)	A	B (μm)^2	C (μm)^4	D (μm)$^{-2}$	E (μm)$^{-4}$
Silicon	0.028	3.41983	0.159906	−0.123109	1.269×10^{-6}	-1.951×10^{-9}
MgO	0.11951	2.95636	0.021958	0	-1.0624×10^{-2}	-2.05×10^{-5}
LiF	0.16733	1.38761	0.001796	-4.1×10^{-5}	-2.3045×10^{-3}	-5.57×10^{-6}
AgCl	0.21413	4.00804	0.079009	0	-8.5111×10^{-4}	-1.976×10^{-7}

Source: Si data from D.F. Edwards and E. Ochoa, *Appl. Optics* **19**, 4130 (1980), others from W. L. Wolfe, The Handbook of Optics, W.G. Driscoll and W. Vaughan, McGraw-Hill, New York, 1978.

for a wide range of semiconductors have been compiled by Madelung in [14]. There are many application-based articles in the literature that provide empirical dispersion relations for a variety of materials; a recent example on far infrared substrates (Ge, Si, ZnSe, ZnS, ZnTe) is given in reference [55]. There are both websites and various journal articles in the literature that give the refractive index of numerous materials as a function of wavelength.

1.3.3 Refractive Index of Semiconductors

1.3.3.1 Refractive Index of Crystalline Semiconductors

A particular interest in the case of semiconductors is in n and K for photon energies greater than the bandgap E_g for optoelectronics applications. Due to various features and singularities in the E-**k** diagrams of crystalline semiconductors, the optical constants n and K for $\hbar\omega > E_g$ are not readily expressible in simple terms. Various authors, for example, Forouhi and Bloomer [42, 56] and Chen et al. [57], have nonetheless provided useful and tractable expressions for modeling n and K in this regime. In particular, Forouhi–Bloomer (FB) equations express n and K in terms of the photon energy $\hbar\omega$ in a consistent way that obey the Kramers–Kronig relations [42], that is

$$K = \sum_{i=1}^{q} \frac{A_i(\hbar\omega - E_g)^2}{(\hbar\omega)^2 - B_i(\hbar\omega) + C_i} \quad \text{and} \quad n = n(\infty) + \sum_{i=1}^{q} \frac{B_{oi}(\hbar\omega) + C_{oi}}{(\hbar\omega)^2 - B_i(\hbar\omega) + C_i}, \tag{1.20}$$

where $(\hbar\omega)$ is the photon energy; q is an integer that represents the number of terms needed to suitably model experimental n, K; E_g is the bandgap and A_i, B_i, C_i, B_{oi}, C_{oi} are constants; B_{oi} and C_{oi} depend on A_i, B_i, C_i, and E_g—only the latter four are independent parameters; and $B_{oi} = (A_i/Q_i)[-(1/2)B_i^2 + E_gB_i - E_g^2 + C_i]$, $C_{oi} = (A_i/Q_i)[(1/2)(E_g^2 + C_i)B_i - 2E_gC_i]$, and $Q_i = (1/2)(4C_i - B_i^2)^{1/2}$. Forouhi and Bloomer provide a table of FB coefficients, A_i, B_i, C_i, and E_g for four terms in the summation in Eq. (1.20) [42] for a number of semiconductors; an example that shows an excellent agreement between the FB dispersion relation and the experimental data is shown in Figure 1.3. Table 1.4 provides the FB coefficients for a few selected semiconductors.

Other useful theoretical or somewhat semiempirical dispersion relationships have also been proposed, for example, by Afromowitz [58], Adachi [59–63], Campi and Papuzza [64], and others [65]. These models have been applied to various semiconductors and their alloys with relative success over certain photon energy ranges. One of the useful and straightforward approaches to modeling the dispersion has been based on writing the complex relative permittivity $\varepsilon_r(\hbar\omega)$ as a finite sum of a number of damped harmonic oscillators (the so-called *harmonic oscillator approximation*), and fitting this expression to the experimental data as in references [66, 67], even though many terms may be needed and the curve fit process has to be carefully chosen to ensure a reliable representation of the data. One of best models considered so far, however, has involved parametric modeling [68–70], in which not only a sum of harmonic oscillators are used but also Gaussian broadened polynomials to represent the dispersion of the complex relative permittivity, and hence n and K.

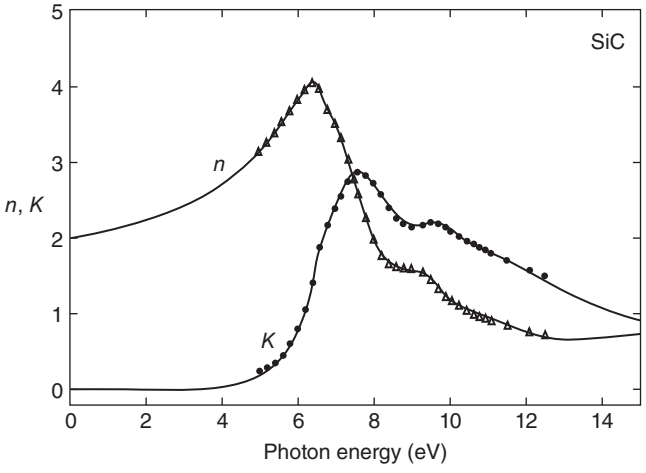

Figure 1.3 *n* and *K* versus photon energy for crystalline SiC. The solid line is obtained from the FB equation with four terms with appropriate parameters, and the points represent the experimental data. See original reference [42] for the data and details. Source: Reprinted with permission, from Figure 2c, A.R. Forouhi and I. Bloomer, Phys. Rev. B, 38, 1865. Copyright (1988) by the American Physical Society.

1.3.3.2 Bandgap and Temperature Dependence

The refractive index of a semiconductor (typically for $\hbar\omega < E_g$) typically decreases with increasing bandgap E_g. There are various empirical and semi-empirical rules and expressions that relate n to E_g. Based on an atomic model, Moss has suggested that n and E_g are related by $n^4 E_g = K =$ constant [71, 72] (K is about ~100 eV). In the Hervé–Vandamme relationship [73],

$$n^2 = 1 + \left(\frac{A}{E_g + B}\right)^2, \tag{1.21}$$

where A and B are constants as $A \approx 13.6$ eV and $B \approx 3.4$ eV. The temperature dependence of n arises from the variation of E_g with the temperature T, and it typically increases with increasing temperature. The temperature coefficient of refractive index (TCRI) of semiconductors can be found from the Hervé–Vandamme relationship as:

$$\text{TCRI} = \frac{1}{n}\cdot\frac{dn}{dT} = -\frac{(n^2-1)^{3/2}}{13.6n^2}\left[\frac{dE_g}{dT} + \frac{dB}{dT}\right] \tag{1.22}$$

where $dB/dT \approx 2.5 \times 10^{-5}$ eV K^{-1}. TCRI is typically found to be positive (n increasing with temperature) and in the range of 10^{-6} to 10^{-4} K^{-1}.

Although Eqs. (1.21) and (1.22) are popular, there are other very useful empirical and semiempirical relationships (see, e.g., [74]), some of which are summarized in Table 1.5 with appropriate references.

1.3.4 Refractive Index of Glasses

The Sellmeier equation with three terms have been found to represent the dispersion of n reasonably well for most glasses and ceramics. The coefficients in the Sellmeier equation have been listed at several websites [44] and handbooks.

Table 1.4 FB coefficients for selected semiconductors [42] for four terms ($i = 1$ to 4).

	A_i	B_i (eV)	C_i (eV^2)	$n(\infty)$	E_g(eV)
Si	0.00405	6.885	11.864	1.950	1.06
	0.01427	7.401	13.754		
	0.06830	8.634	18.812		
	0.17488	10.652	29.841		
Ge	0.08556	4.589	5.382	2.046	0.60
	0.21882	6.505	11.486		
	0.02563	8.712	19.126		
	0.07754	10.982	31.620		
GaP	0.00652	7.469	13.958	2.070	2.17
	0.14427	7.684	15.041		
	0.13969	10.237	26.567		
	0.00548	13.775	47.612		
GaAs	0.00041	5.871	8.619	2.156	1.35
	0.20049	6.154	9.784		
	0.09688	9.679	23.803		
	0.01008	13.232	44.119		
GaSb	0.00268	4.127	4.267	1.914	0.65
	0.34046	4.664	5.930		
	0.08611	8.162	17.031		
	0.02692	11.146	31.691		
InP	0.20242	6.311	10.357	1.766	1.27
	0.02339	9.662	23.472		
	0.03073	10.726	29.360		
	0.04404	13.604	47.602		
InAs	0.18463	5.277	7.504	1.691	0.30
	0.00941	9.130	20.934		
	0.05242	9.865	25.172		
	0.03467	13.956	50.062		
InSb	0.00296	3.741	3.510	1.803	0.12
	0.22174	4.429	5.447		
	0.06076	7.881	15.887		
	0.04537	10.765	30.119		

Note: First entry in the box is for $i = 1$, and the fourth is for $i = 4$.

Gladstone–Dale formula [82, 83] is an empirical equation that allows the average refractive index n of an oxide glass to be calculated from its density ρ and its constituents as:

$$\frac{n-1}{\rho} = p_1 k_1 + p_2 k_2 + \cdots = \sum_{i=1}^{N} p_i k_i = C_{\mathrm{GD}}, \tag{1.23}$$

Table 1.5 Various selected simple relationships proposed between n and the bandgap E_g.

Relationship	Comment/Reference
$n^4E_g = K$; K = constant	Widely used, but has limitations. $K \approx 95$ eV; 173 eV for Group IV elements [75]; $K = 108$ eV [76]. For a theoretical derivation and discussion of Moss's rule, see [77].
$n^2 = 1 + \left(\frac{A}{E_g + B}\right)^2$	$A \approx 13.6$ eV and $B \approx 3.4$ eV. Hervé–Vandamme relationship. See text.
$n = 4.084 + \beta E_g$	$\beta = -0.62\ \text{eV}^{-1}$. Proposed by Ravindra et al. [76], but has serious limitations for small and large n.
$n = -\ln(0.027E_g)$	The Reddy Equation [78]. Based on the Duffy relationship $E_g = 3.72\Delta\chi_{\text{op}}$ [79] and $\Delta\chi_{\text{op}} = 9.8\exp(-n)$ in [80], where $\Delta\chi_{\text{op}}$ is optical electronegativity.
$n^2 = \frac{12.417}{\sqrt{E_g - 0.365}}$	See [81]. Equivalent to $n^4(E_g - 0.365\ \text{eV}) = 154$. Similar to the Moss relation. $E_g > 0.365$ eV

Note: E_g is in eV.

where the summation is for various oxide components (each a simple oxide), p_i is the weight fraction of the i-th oxide in the compound, and k_i is the refraction coefficient that represents the polarizability of the i-th oxide. The right-hand side of Eq. (1.23) is called the *Gladstone–Dale* coefficient C_{GD}. In more general terms, as a mixture rule for the overall refractive index, the Gladstone–Dale formula is frequently written as:

$$\frac{n-1}{\rho} = \frac{n_1 - 1}{\rho_1} w_1 + \frac{n_2 - 1}{\rho_2} w_2 + \cdots, \tag{1.24}$$

where n and ρ are the effective refractive index and effective density, respectively, of the whole mixture; $n_1, n_2, \ldots$ are the refractive indices of the constituents; $\rho_1, \rho_2, \ldots$ represent the density of each constituent; and $w_1, w_2 \ldots$ are the weight fractions of the constituents. Gladstone–Dale equations for the polymorphs of SiO_2 and TiO_2 give the average n, respectively, as:

$$n(SiO_2) = 1 + 0.21\rho \text{ and } n(TiO_2) = 1 + 0.40\rho \tag{1.25}$$

It is generally assumed that the refractive index can be related to the polarizability α through the well-known Lorentz–Lorenz equation (equivalent to the Clausius–Mossotti equation in dielectrics), which involves the local field as

$$\frac{n^2 - 1}{n^2 + 2} = \frac{1}{3\varepsilon_o} \sum_j N_j \alpha_j \tag{1.26}$$

in which α_j is the polarizability of a given type (species) (j) of atoms in the structure, and N_j is the concentration of this species of atoms. Equation (1.26) includes both electronic and ionic polarizability and assumes that the local field is the Lorentz field, which depends on polarization through $P/3\varepsilon_o$ in the standard model for cubic crystals and noncrystalline solids. Ritland [84] assumed that the local field depends on the polarization as bP/ε_o, where b is a numerical constant, and reformulated Eq. (1.26) in SI units

as

$$\frac{n^2-1}{n^2-1+(1/b)} = \frac{b}{\varepsilon_o}\sum_j N_j\alpha_j \tag{1.27}$$

and b is kept as a variable fitting parameter to the experimental data. Obviously, $b = 1/3$ is the usual Lorentz–Lorenz equation, but the best fits do not necessarily lead to 1/3 [84]. Most recent work on the refractive index of glasses has invariably used the Sellmeier equation, given its excellent fit to the dispersion data on glasses, as well as the adoption of the Sellmeier equation by some industrial glass manufacturers such as Schott [85]. Further, in some cases, the temperature dependence of the Sellmeier coefficients are also evaluated, so that dn/dT can be determined at different wavelengths [86–90]. While dn/dT is positive for many semiconductors, this is not generally true for glasses.

1.3.5 Wemple–DiDomenico Dispersion Relation

Based on the single oscillator model, the Wemple–DiDomenico (WD) model is a semi-empirical dispersion relation for determining the refractive index at photon energies below the interband absorption edge in a variety of materials [91, 92]. It is given by

$$n^2 = 1 + \frac{E_o E_d}{E_o^2 - (h\nu)^2}, \tag{1.28}$$

where ν is the frequency, h is the Planck constant, E_o is the single oscillator energy, and E_d is the dispersion energy, which is a measure of the average strength of interband optical transition. E_d can be written as $E_d = \beta N_c Z_a N_e$ (eV), where N_c is the effective coordination number of the cation nearest-neighbor to the anion (e.g. $N_c = 6$ in NaCl, $N_c = 4$ in Ge), Z_a is the formal chemical valency of the anion ($Z_a = 1$ in NaCl, 2 in Te, and 3 in GaP), N_e is the effective number of valence electrons per anion excluding the cores ($N_e = 8$ in NaCl, Ge; 10 in TlCl; 12 in Te; $9^1/_3$ in As_2Se_3), and β is a constant that depends on whether the interatomic bond is ionic (β_i) or covalent (β_c): $\beta_i = 0.26 \pm 0.04$ eV (e.g. halides NaCl, ThBr, etc., and most oxides, Al_2O_3, etc.), and $\beta_c = 0.37 \pm 0.05$ eV (e.g. tetrahedrally bonded $A^N B^{8-N}$ zinc blende and diamond type structures, GaP, ZnS, etc., and wurtzite crystals have a β that is intermediate between β_i and β_c). Further, empirically, $E_o = CE_g$(D), where E_g(D) is the *lowest* direct bandgap and C is a constant, typically $C \approx 1.5$. E_o has been associated with the main peak in the $\varepsilon_r''(h\nu)$ versus $h\nu$ spectrum. The parameters required for calculating n from Eq. (1.28) are listed in Table 1.6 [91]. It should be apparent that one can improve on the single oscillator model by adding a second oscillator term to Eq. (1.28) [93], and so on; although one loses the simplicity of the model, which the experimentalists like.

Since its publication in 1971, the WD model has also been successfully applied to various amorphous semiconductors and glasses in addition to crystals, following the original arguments of Wemple [92]. In their original work, WD provided the single oscillator parameters for an extensive list of materials, some of which are summarized in Table 1.6, with further discussion in [94]. The ratio E_o/E_g has been observed by researchers to be very roughly in the range 1.5–2.5. The simple WD model is expected to hold in the small absorption region of the spectrum, that is, away from absorption bands due to interband transitions ($h\nu < E_g$) or Reststrahlen absorption, etc. While it is apparent that the

Table 1.6 Examples of parameters for Wemple–DiDomenico dispersion relationship in various materials.

Material	N_c	Z_a	N_e	E_o (eV)	E_d (eV)	β (eV)	β	Comment
NaCl	6	1	8	10.3	13.6	0.28	β_i	Halides, LiF, NaF, etc.
CsCl	8	1	8	10.6	17.1	0.27	β_i	CsBr, CsI, etc.
TlCl	8	1	10	5.8	20.6	0.26	β_i	TlBr
CaF_2	8	1	8	15.7	15.9	0.25	β_i	BaF_2, etc.
CaO	6	2	8	9.9	22.6	0.24	β_i	Oxides, MgO, TeO_2, etc.
Al_2O_3	6	2	8	13.4	27.5	0.29	β_i	
$LiNbO_3$	6	2	8	6.65	25.9	0.27	β_i	
TiO_2	6	2	8	5.24	25.7	0.27	β_i	
ZnO	4	2	8	6.4	17.1	0.27	β_i	
ZnSe	4	2	8	5.54	27	0.42	β_c	II-VI, Zinc blende, ZnS, ZnTe, CdTe
GaAs	4	3	8	3.55	33.5	0.35	β_c	III-V, Zinc blende, GaP, etc.
Si (Crystal)	4	4	8	4.0	44.4	0.35	β_c	Diamond, covalent bonding; C (diamond), Ge, β-SiC, etc.
SiO_2 (Crystal)	4	2	8	13.33	18.10	0.28	β_i	Average crystalline form
SiO_2 (Amorphous)	4	2	8	13.38	14.71	0.23	β_i	Fused silica
CdSe	4	2	8	4.0	20.6	0.32	β_i–β_c	Wurtzite

Note: Values extracted and combined from tables in [91].

WD relation can only be approximate, it has nonetheless found wide acceptance among experimentalists due to its straightforward simplicity. For example, in 2018 alone, it has been applied nearly 200 times to a wide variety of inorganic and organic material systems, particularly to semiconductor films.

1.3.6 Group Index

Group index is a factor by which the group velocity of a group of waves in a dielectric medium is reduced with respect to propagation in free space. It is denoted by N_g and defined by $N_g = v_g/c$, where v_g is the group velocity, defined by $v_g = d\omega/dk$, where k is the wave vector or the propagation constant. The group index can be determined from the ordinary refractive index n through [95]

$$N_g = n - \lambda \frac{dn}{d\lambda} \tag{1.29}$$

where λ is the wavelength of light (in free space). Figure 1.4 illustrates the relation between N_g and n in SiO_2. The group index N_g is the quantity that is normally used in calculating dispersion in optical fibers, since it is N_g that determines the group velocity of a propagating light pulse in a glass or transparent medium. It should be remarked that, although n vs. λ can decrease monotonically with λ over a range of wavelengths, N_g can exhibit a minimum in the same range where the dispersion, $dN_g/d\lambda$, becomes zero. The point $dN_g/d\lambda = 0$ is called the *zero-material dispersion wavelength*, which is around 1300 nm for silica, as apparent in Figure 1.4.

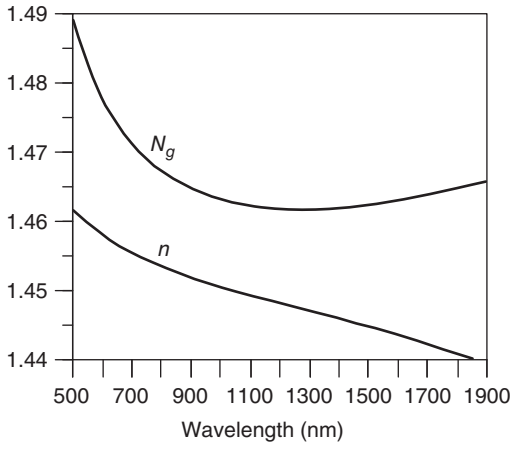

Figure 1.4 Refractive index n and the group index N_g of pure SiO_2 (silica) glass as a function of wavelength. Source: Adapted from S.O. Kasap, 2017 [30].

1.4 The Swanepoel Technique: Measurement of n and α for Thin Films on Substrates

1.4.1 Uniform Thickness Films

In many instances, the optical constants are conveniently measured by examining the transmission through a thin film of the material deposited on a transparent glass or other (e.g. sapphire) substrate. The classic reference on the optical properties of thin films has been the book by Heavens [96]; the book is still useful in clearly describing what experiments can be carried out, and has a number of useful derivations such as the reflectance and transmittance through thin films in the presence of multiple reflections. Since then, numerous research articles and reviews have been published. Poelman and Smet [97] have critically reviewed how a single transmission spectrum measurement can be used to extract the optical constants of a thin film. In general, the amount of light that gets transmitted through a thin film material depends on the amount of reflection and absorption that takes place along the light path. If the material is a thin film with a moderate absorption coefficient α, then there will be multiple interferences at the transmitted side of the sample, as illustrated in Figure 1.5.

In this case, some interference fringes will be evident in the transmission spectrum obtained from a spectrophotometer, as shown in Figure 1.6. One very useful method that makes use of these interference fringes to determine the optical properties of the material is called the *Swanepoel method* [98] which is based on earlier works of Manifacier et al. [99] and Hall and Ferguson [100].

Swanepoel has shown that the optical properties of a uniform thin film of thickness d, refractive index n, and absorption coefficient α, deposited on a thick substrate with a refractive index s, as shown in Figure 1.5, can be obtained from the transmittance T given by

$$T = \frac{Ax}{B - Cx\cos\varphi + Dx^2} \tag{1.30}$$

where $A = 16n^2s$, $B = (n+1)^3(n+s^2)$, $C = 2(n^2-1)(n^2-s^2)$, $D = (n-1)^3(n-s^2)$, $\varphi = 4\pi nd/\lambda$, $x = \exp(-\alpha d)$ is an absorbance-type parameter, and n, s, and α are all

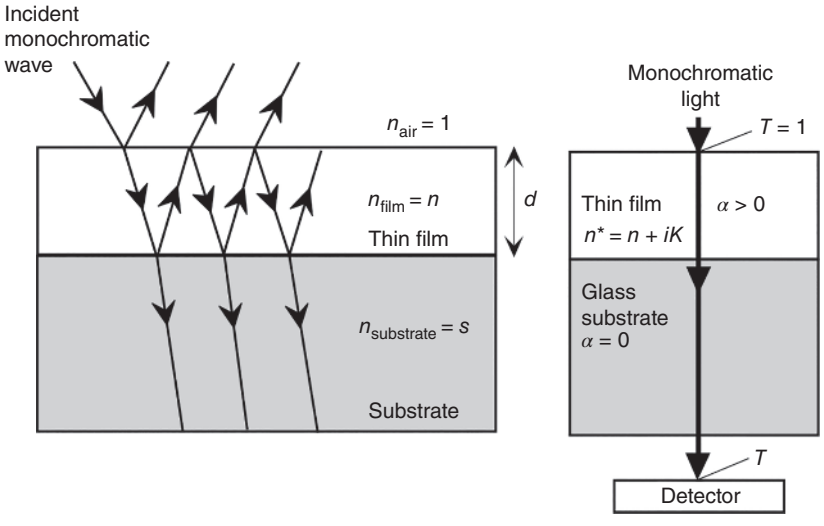

Figure 1.5 Schematic sketch of the typical behavior of light passing through a thin film on a substrate. On the left, oblique incidence is shown to demonstrate the multiple reflections. In most measurements, the incident beam is nearly normal to the film, as shown on the right.

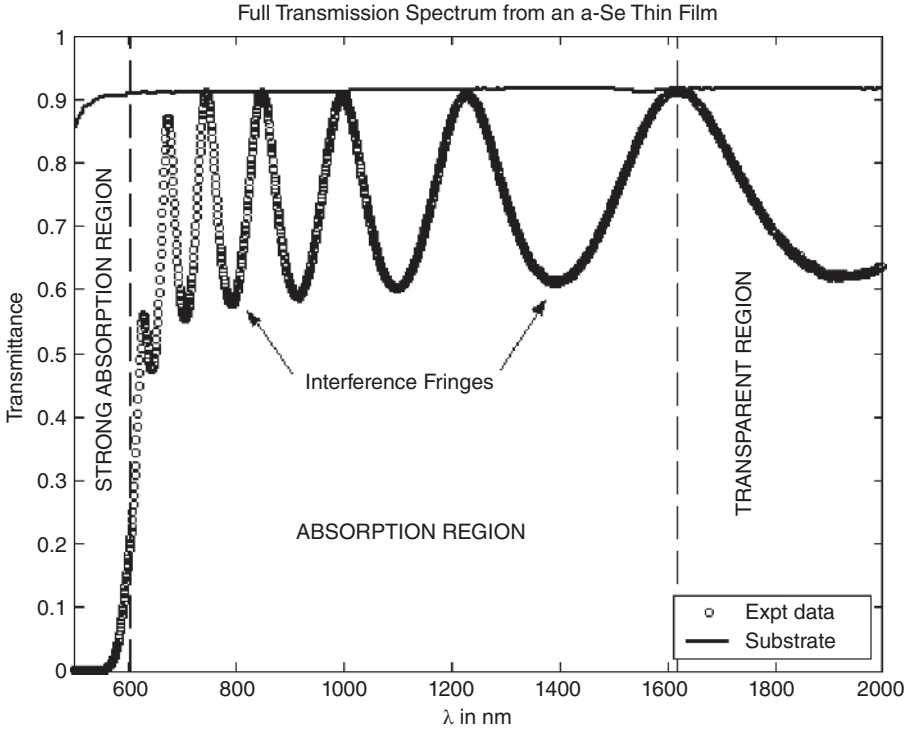

Figure 1.6 An example of a typical transmission spectrum of a 0.969-μm-thick amorphous Se thin film that has been vacuum coated on a glass substrate held at a substrate temperature of 50°C during the deposition.

functions of wavelength λ. Although x (with values of 1 under no absorption and approaching 0 under strong absorption) has been called "absorbance" in most studies using the Swanepoel technique as in the original papers, the usual definition of absorbance, however, is $\log_{10}(1/T)$, so that x, strictly, is not true absorbance. Eq. (1.30) assumes $K^2 << n^2$, where $n + iK$ is the complex refractive index of the film and normal incidence. What is very striking and useful is that all the important optical properties can be determined from the application of this equation; this will be introduced in the subsequent paragraphs. Before the optical properties of any thin film can be extracted, the refractive index of their substrate must first be calculated. For a glass substrate with very negligible absorption, that is, $K \leq 0.1$ and $\alpha \leq 10^{-2}$ cm^{-1}, in the range of operating wavelengths, the refractive index s is,

$$s = \frac{1}{T_s} + \sqrt{\left(\frac{1}{T_s^2} - 1\right)} \tag{1.31}$$

where T_s is the transmittance value measured from the spectrophotometer. This expression can be derived from the transmittance equation for a bulk sample with little attenuation. With this refractive index s known, the next step is to construct two envelopes around the maxima and minima of the interference fringes in the transmission spectrum, as indicated in Figure 1.7.

There will altogether be two envelopes that have to be constructed before any of the expressions derived from Eq. (1.30) can be used to extract the optical properties. This

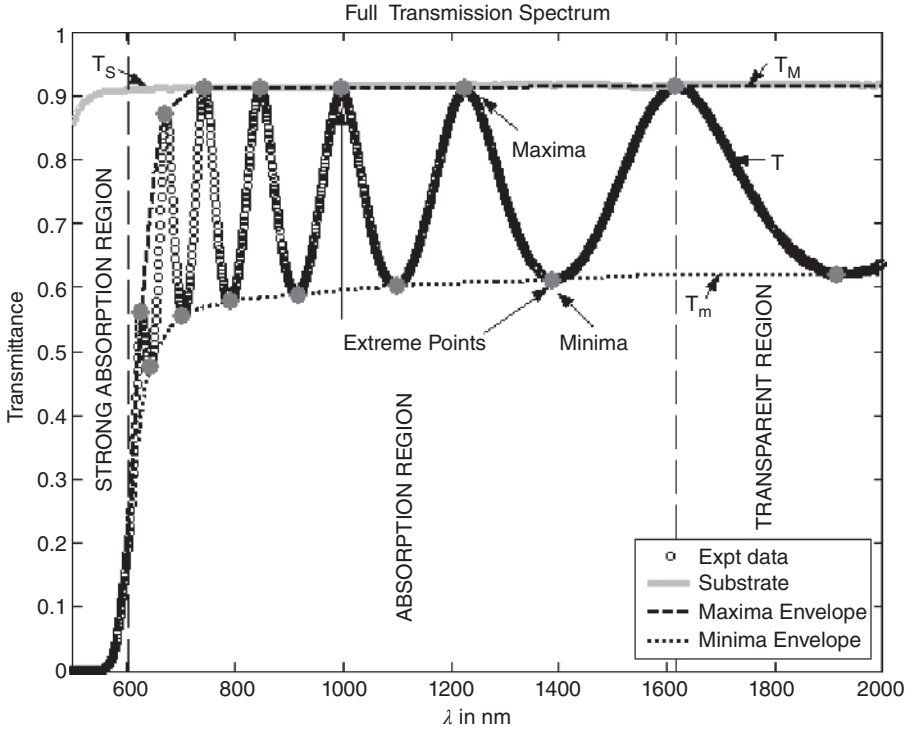

Figure 1.7 The construction of envelopes in the transmission spectrum of the thin a-Se film in Figure 1.6.

can be done by locating all the extreme points of the interference fringes in the transmission spectrum and then making sure that the respective envelopes, $T_{\mathrm{M}}(\lambda)$ for the maxima and $T_{\mathrm{m}}(\lambda)$ for the minima, pass through these extremes, the maxima and minima, of $T(\lambda)$ tangentially. From Eq. (1.30), it is not difficult to see that, at $\cos\varphi = \pm 1$, the expressions that describe the two envelopes are,

$$\text{Maxima}: T_M = \frac{Ax}{B - Cx + Dx^2}, \tag{1.32a}$$

$$\text{Minima}: T_m = \frac{Ax}{B + Cx + Dx^2}. \tag{1.32b}$$

Figure 1.7 shows two envelopes constructed for a transmission spectrum of an a-Se thin film. It can also be seen that the transmission spectrum is divided into three special regions according to their transmittance values: (i) the *transparent region*, where $T(\lambda) \geq 99.99\%$ of the substrate's transmittance value of $T_s(\lambda)$, (ii) the *strong absorption region*, where $T(\lambda)$ is typical smaller than 20%, and (iii) the *absorption region*, in between the two latter regions as shown in Figure 1.7.

The refractive index of the thin film can be calculated from the two envelopes, $T_M(\lambda)$ and $T_m(\lambda)$, and the refractive index of the substrate s through

$$n = \left[N + (N^2 - s^2)^{1/2}\right]^{1/2}; \; N = 2s\left[\frac{T_M - T_m}{T_M T_m}\right] + \frac{s^2 + 1}{2}, \tag{1.33}$$

where N is defined by the second equation on the right hand side of Eq. (1.33). T_M and T_m are assumed to be continuous functions of λ and x, so that values have to be at the same wavelength for use in Eq. (1.33). The derivation of Eq. (1.33) is based on considering $1/T_m - 1/T_M$, which is $2C/A$, and then substituting for C and A from earlier, and then solving for n. Since the equation is not valid in the strong absorption region, where there are no maxima and minima, the calculated refractive index has to be fitted to a well-established dispersion model for extrapolation to shorter wavelengths before it can be used to obtain other optical constants. Usually either the Sellmeier or the Cauchy dispersion equation is used to fit n vs λ experimental data in this range. Figure 1.8 shows the refractive indices extracted from the envelopes and fitted to the Sellmeier dispersion model with two terms.

With the refractive index of the thin film corresponding to two adjacent maxima (or minima) at points 1 and 2, given as n_1 at λ_1 and n_2 at λ_2, the thickness can be easily calculated from the basic interference equation of waves as follows:

$$d_{\text{crude}} = \frac{\lambda_1 \lambda_2}{2(\lambda_1 n_2 - \lambda_2 n_1)} \tag{1.34}$$

where d_{crude} refers to the thickness obtained from the maxima (minima) at points 1, 2. As other adjacent pairs of maxima or minima points are used, more thickness values can be deduced, and hence an average value calculated. It is assumed the film has an ideal uniform thickness.

The absorption coefficient α can be obtained once x is extracted from the transmission spectrum. This can be done as follows:

$$\alpha = -\frac{\ln(x)}{d_{\text{ave}}} \tag{1.35}$$

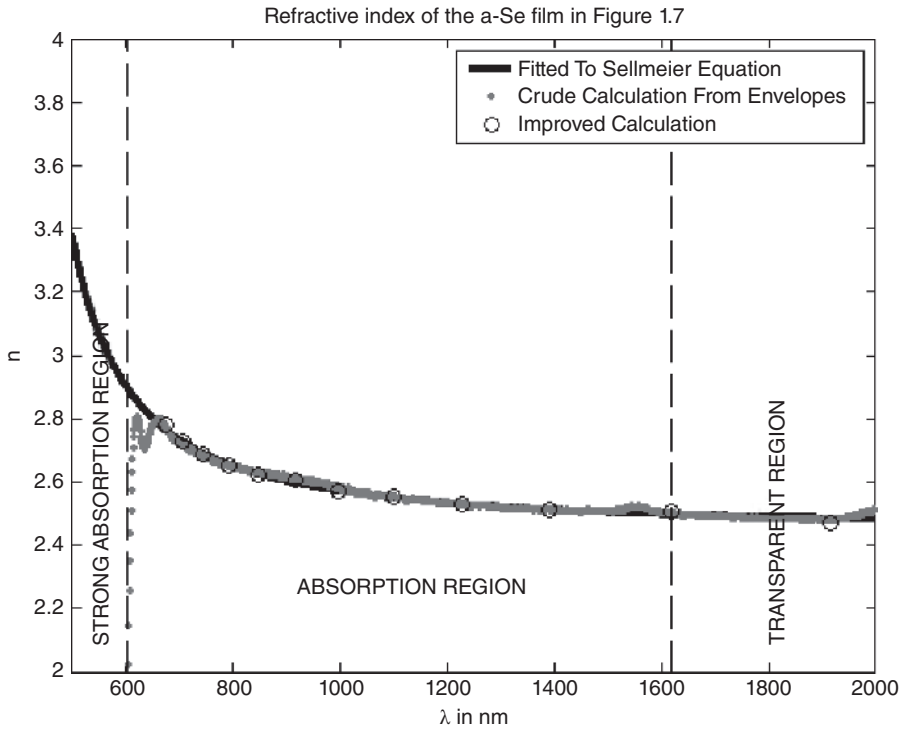

Figure 1.8 Determination of the refractive index from the transmission spectrum maxima and minima shown in Figure 1.7. The solid black curve shows the fitted Sellmeier n vs. λ curve, which follows $n^2 = 3.096 + 2.943\lambda^2/[\lambda^2 - (402.31)^2]$, where λ is in nm.

where $x = \frac{E_M - \sqrt{E_M^2 - (n^2-1)^3(n^2-s^4)}}{(n-1)^3(n-s^2)}$; $E_M = \frac{8n^2 s}{T_M} + (n^2-1)(n^2-s^2)$; and d_{ave} is the average thickness of d_{crude}.

The accuracy of the thickness, the refractive index, and the absorption coefficient can all be further improved in the following manner. The first step is to determine a new set of interference orders, represented by m', for the interference fringes from the basic interference equation of waves; that is,

$$m' = \frac{2n_e d_{\text{ave}}}{\lambda_e}, \tag{1.36a}$$

where n_e and λ_e are values taken at any extreme point, and m' is an integer if the extremes taken are maxima or a half-integer if the extremes taken are minima.

The second step is to get a new corresponding set of thickness values, d', from this new set of order numbers m', by rearranging Eq. (1.36a) as:

$$d' = \frac{m'\lambda_e}{2n_e} \tag{1.36b}$$

From this new set of thickness values, d', a new average thickness, d_{new}, must be calculated before it can be applied to improve the refractive index. This can be done by

ignoring those d' that have values very different from the rest during averaging. With this new average thickness, a more accurate refractive index n_e can be obtained from the same equation,

$$n_e = \frac{m'\lambda_e}{2d_{\text{new}}} \tag{1.36c}$$

This new refractive index can then be fitted to the previous dispersion model again, so that an improved absorption coefficient α can be calculated from Eq. (1.35). All these parameters can then be used in Eq. (1.30) to regenerate a calculated transmission spectrum $T_{\text{cal}}(\lambda)$, so that the root mean square error (RMSE) can be determined from the experimental spectrum T_{exp}. The RMSE is calculated as follows:

$$\text{RMSE} = \sqrt{\frac{\sum_{i=1}^{q}(T_{\text{exp}} - T_{\text{cal}})^2}{q}}, \tag{1.37}$$

where T_{exp} is the transmittance of the experimental or measured spectrum, T_{cal} is the transmittance of the regenerated spectrum obtained through the Swanepoel calculation method, and q is the range of the measurement. Figure 1.9 shows the regenerated transmission spectrum of the a-Se thin film that appeared in Figure 1.6 using the optical constants calculated from the envelopes (as quoted in the caption of Figure 1.8).

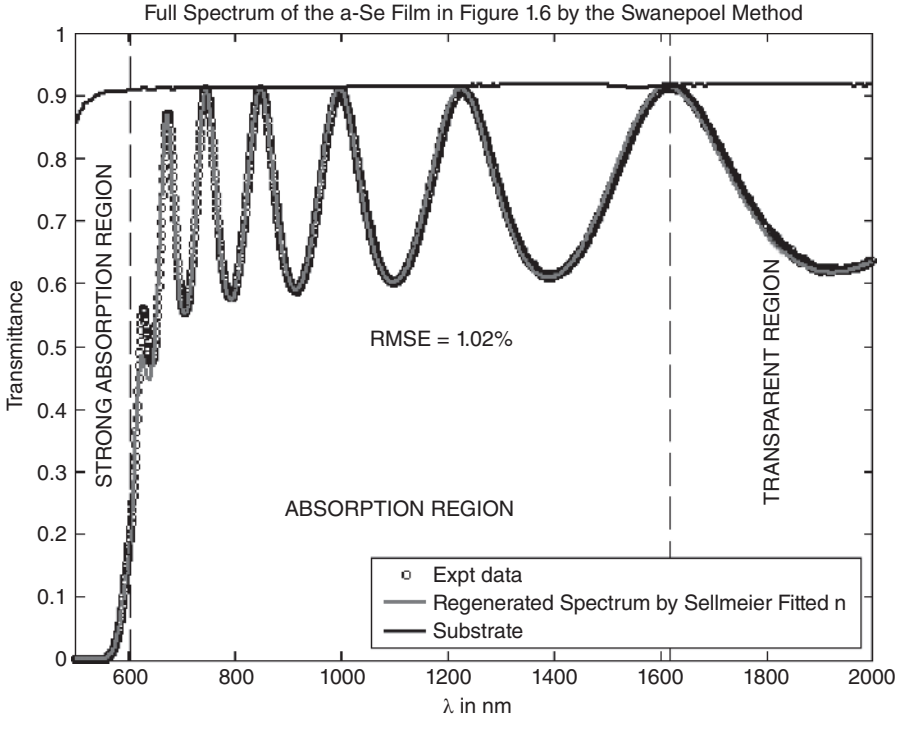

Figure 1.9 Regenerated transmission spectrum of the sample in Figure 1.6.

1.4.2 Thin Films with Non-uniform Thickness

The Swanepoel technique in the case of a film with a wedge-like cross-section, as shown in Figure 1.10, involves the integration of Eq. (1.30) over the thickness of the film in order for it to more accurately describe the transmission spectrum [101]. The transmittance then becomes,

$$T_{\Delta d} = \frac{1}{\varphi_2 - \varphi_1} \int_{\varphi_1}^{\varphi_2} \frac{Ax}{B - Cx\cos\varphi + Dx^2} dx \tag{1.38}$$

with

$$\varphi_1 = \frac{4\pi n(\overline{d} - \Delta d)}{\lambda}, \text{ and } \varphi_2 = \frac{4\pi n(\overline{d} + \Delta d)}{\lambda},$$

where $A = 16n^2 s$, $B = (n+1)^3(n+s^2)$, $C = 2(n^2-1)(n^2-s^2)$, $D = (n-1)^3(n-s^2)$, φ has been defined after Eq. (1.30), $x = \exp(-\alpha\overline{d})$ corresponds x to the absorbance-type parameter calculated using the average film thickness $\overline{d}$ over the illumination region, n and s are the refractive index of the film and substrate, respectively, α is the absorption coefficient, and Δd is the *thickness variation* throughout the illumination area, which has been called the *roughness* of the film (This nomenclature is actually confusing, since the film may not be truly "rough," but may just have a continuously increasing thickness as in a wedge from one end to the other.)

The first parameter to be extracted before the rest of the optical properties is Δd. Consider the transmission region where absorption is very small, that is, x is almost unity, and the spectrum exhibits clear maxima and minima. Eq. (1.38) can be modified by considering the maxima and minima, which are both continuous functions of λ. In this way, we have,

$$\text{Maxima}: T_{Md} = \frac{\lambda}{2\pi n\Delta d} \frac{a}{\sqrt{1-b^2}} \tan^{-1}\left[\frac{1+b}{\sqrt{1-b^2}} \tan\left(\frac{2\pi n\Delta d}{\lambda}\right)\right], \tag{1.39a}$$

$$\text{Minima}: T_{md} = \frac{\lambda}{2\pi n\Delta d} \frac{a}{\sqrt{1-b^2}} \tan^{-1}\left[\frac{1-b}{\sqrt{1-b^2}} \tan\left(\frac{2\pi n\Delta d}{\lambda}\right)\right], \tag{1.39b}$$

where $a = \frac{A}{B+D}$, and $b = \frac{C}{B+D}$.

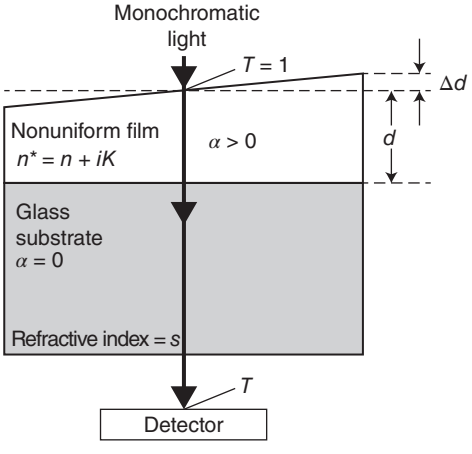

Figure 1.10 System of an absorbing thin film with a variation in thickness on a thick finite transparent substrate.

Notice that there is no x in these equations, since $x = 1$ was used. As long as $0 < \Delta d < \lambda/4n$, the refractive index, n and Δd, can both can be obtained by simultaneously solving Eqs. (1.39a) and (1.39b) numerically at various wavelengths.

Since Eqs. (1.39a) and (1.39b) are only valid in the region of zero absorption, the refractive index, outside of the transparent region, must be obtained in another way. Theoretically, a direct integration of Eq. (1.38) over both Δd and x can be performed, although this would be analytically too difficult. Nevertheless, over the wavelength region where absorption is small (where one can still distinguish interference fringes), an approximation to the integration, according to Swanepoel, is as follows:

$$\text{Maxima}: T_{Mx} = \frac{\lambda}{2\pi n \Delta d} \frac{a_x}{\sqrt{1-b_x^2}} \tan^{-1}\left[\frac{1+b_x}{\sqrt{1-b_x^2}} \tan\left(\frac{2\pi n \Delta d}{\lambda}\right)\right], \tag{1.40a}$$

$$\text{Minima}: T_{mx} = \frac{\lambda}{2\pi n \Delta d} \frac{a_x}{\sqrt{1-b_x^2}} \tan^{-1}\left[\frac{1-b_x}{\sqrt{1-b_x^2}} \tan\left(\frac{2\pi n \Delta d}{\lambda}\right)\right], \tag{1.40b}$$

where $a_x = \frac{Ax}{B+Dx^2}$ and $b_x = \frac{Cx}{B+Dx^2}$. As long as $0 < x \leq 1$, numerically, there will only be one unique solution. Therefore, the two desired optical properties, refractive index, n and x (and hence α), can both be obtained when Eqs. (1.40a) and (1.40b) are solved simultaneously using the calculated average Δd. Eqs. (1.40a) and (1.40b) are valid for $\Delta d \ll \overline{d}$.

As before, the calculated refractive index can be fitted to a well-established dispersion model, such as the Cauchy or Sellmeier equation, as shown in Figure 1.11, for

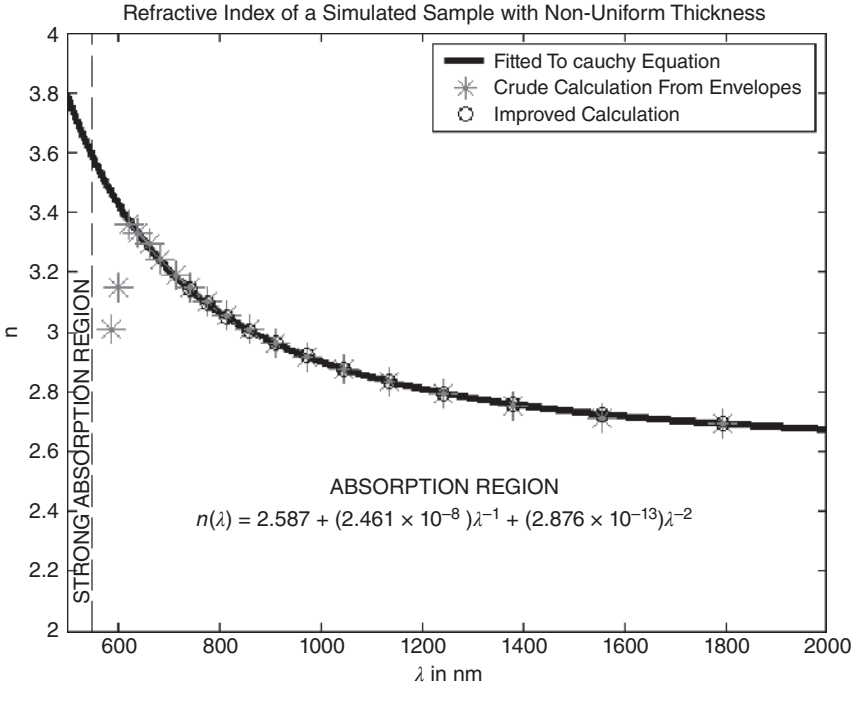

Figure 1.11 The refractive index of a sample with $\overline{d} = 1$ μm and $\Delta d = 30$ nm, and n fitted to a Cauchy equation in the figure. Eqs. (1.40a) and (1.40b) were used for the determination of n.

extrapolation to shorter wavelengths. The thickness is calculated from any two adjacent maxima (or minima) using Eq. (1.34), and the absorption coefficient can be calculated from

$$\alpha_{\text{weak}} = -\frac{\ln(x_{\text{weak}})}{\overline{d}} \tag{1.41}$$

where α_{weak} is the absorption coefficient in the weak and medium absorption region; x_{weak} is the absorbance-like parameter (x) obtained from Eqs. (1.40a) and (1.40b); and $\overline{d}$, as before, is the average thickness.

According to Swanepoel, in the region of strong absorption, the interference fringes are smaller, and the spectrum approaches the interference-free transmission sooner. Since the transmission spectra in this region are the same for any film with the same average thickness, regardless of its uniformity, the absorption coefficient in the strong absorption region will thus be,

$$\alpha_{\text{strong}} = -\frac{\ln(x_{\text{strong}})}{\overline{d}} \tag{1.42}$$

where $x_{\text{strong}} = \frac{A-\sqrt{(A^2-4T_i^2BD)}}{2T_iD}$, $T_i = \frac{2T_MT_m}{T_M+T_m}$, and T_M and T_m are the envelopes of maxima and minima, respectively, constructed from the measured spectrum.

The accuracy of the thickness and refractive index can be further improved in exactly the same way as that for a film with uniform thickness for the computation of the new absorption coefficient, using Eqs. (1.40a) and (1.40b). Figure 1.12 shows the regenerated

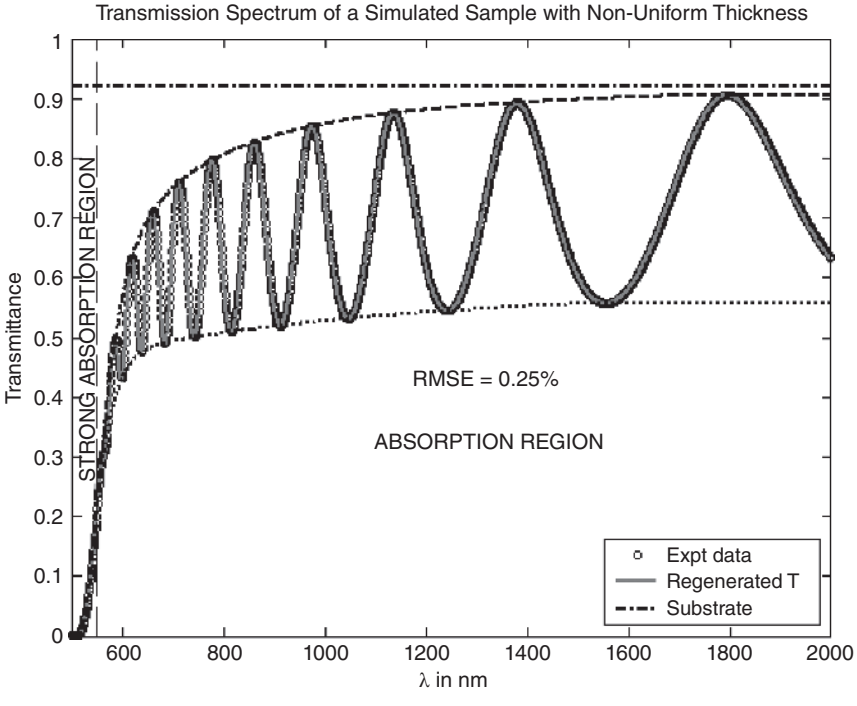

Figure 1.12 A regenerated transmission spectrum of a sample with an average thickness of 1 μm and average Δd of 30 nm, and a refractive index fitted to a Cauchy equation in Figure 1.11.

transmission spectrum of a simulated sample with nonuniform thickness using the optical constants calculated from the envelopes. Marquez et al. [102] have discussed the application of Swanepoel technique to wedge-shaped As_2S_3 thin film and made use of the fact that a non-uniform wedge-shaped thin film has a compressed transmission spectrum. Figure 1.13 shows a flow chart that highlights the various steps involved in the extraction of the optical coefficients of thin film for both uniform and a nonuniform film thicknesses.

Various computer algorithms based on the Swanepoel technique are available in the literature [103]. Further discussions and enhancements are also available [97, 104–106]. For example, one improvement in the strong absorption region is based on a so-called tangencypoint method as described in [106]. There are numerous useful applications of the Swanepoel technique for extracting the optical constants of thin films; some selected recent examples are given in [107–118].

1.5 Transmittance and Reflectance of a Partially Transparent Plate

The transmittance of the thin film in Figure 1.6 is based on the interference of light waves within the thin film; it assumes that waves have a much longer coherence length than the thickness of the film, so that we may suitably add the optical fields of the waves. A film would be too thick if the coherence length of the waves is shorter than the thickness of the film. When we pass light through a transparent (or partially transparent) plate, we typically do not observe interference effects. Even if we have a thin film, we may not observe interference effects if the light source is incoherent. In these cases, we cannot add the electric fields to calculate the reflected and transmitted light irradiances; instead, we need to use reflectance and transmittance of the surfaces. Consider the multiple reflections shown in Figure 1.14. The first transmitted light intensity into the plate is $(1-R)$, and the first transmitted light out is $(1-R)(1-R) = (1-R)^2$. However, there are internal reflections, so that the second transmitted light is $R^2(1-R)^2$, so that the transmitted intensity through the plate is $T_{\text{plate}} = (1-R)^2[1+R^2+R^4+\ldots]$, or

$$T_{\text{plate}} = \frac{(1-R)^2}{1-R^2} = \frac{1-R}{1+R} = \frac{2nn_o}{n^2+n_o^2} \tag{1.43}$$

where $R = (n-n_o)/(n+n_o)$, and n is the refractive index of the plate and n_o that of the surrounding, as in Figure 1.14. One of the simplest ways to determine the refractive index of a medium as a plate is to measure the transmittance T_{plate}, and then use

$$\frac{n}{n_o} = T_{\text{plate}}^{-1} + \sqrt{T_{\text{plate}}^{-2} - 1} \tag{1.44}$$

The overall reflectance is $1 - T_{\text{plate}}$, so that

$$R_{\text{plate}} = \frac{(n-n_o)^2}{n^2+n_o^2} \tag{1.45}$$

If the plate is partially transparent with some attenuation coefficient α, then, each time light traverses the thickness L of the plate, it experiences an attenuation factor $\exp(-\alpha L)$,

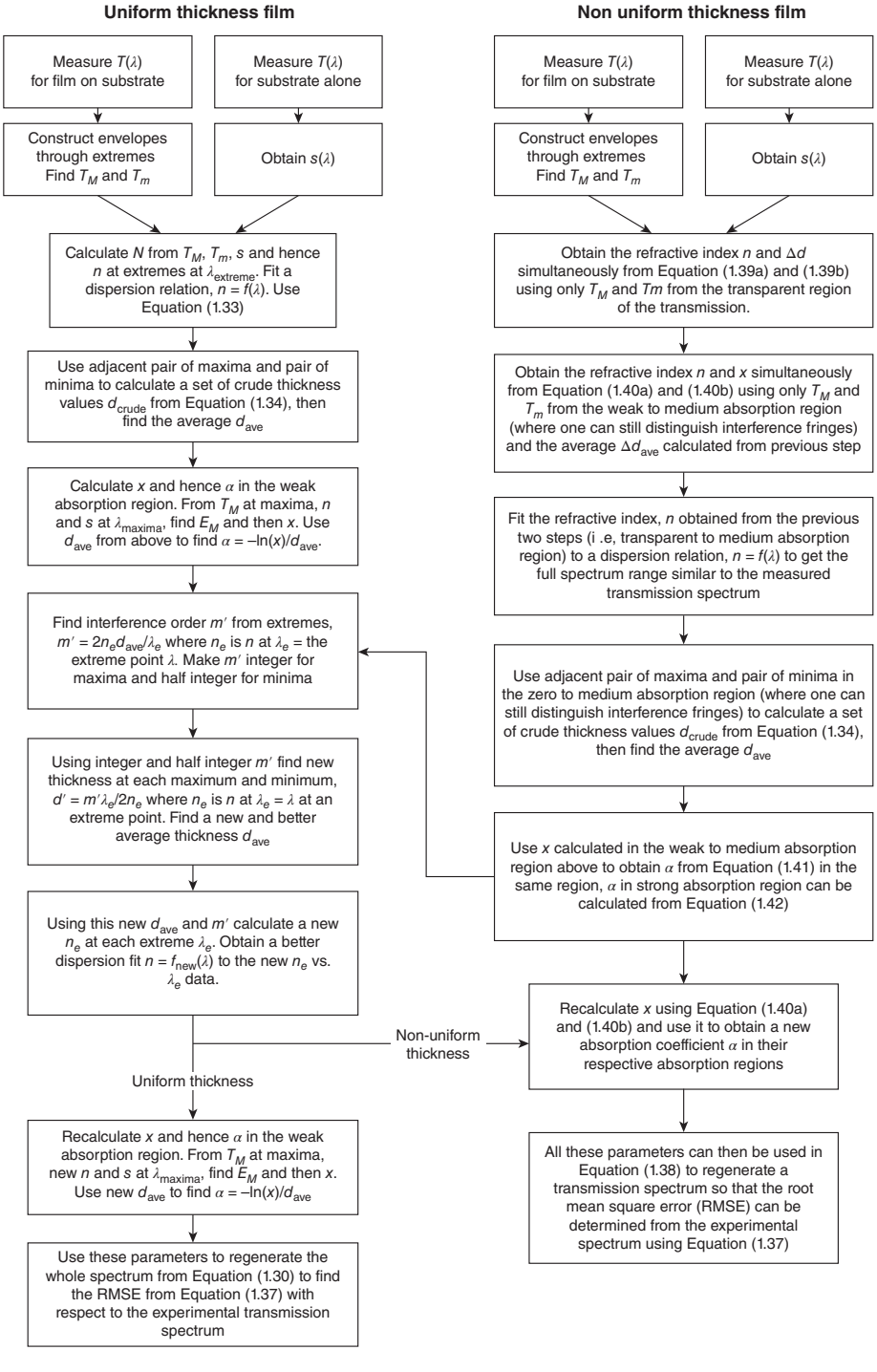

Figure 1.13 A flow chart highlighting the steps involved in the Swanepoel technique.

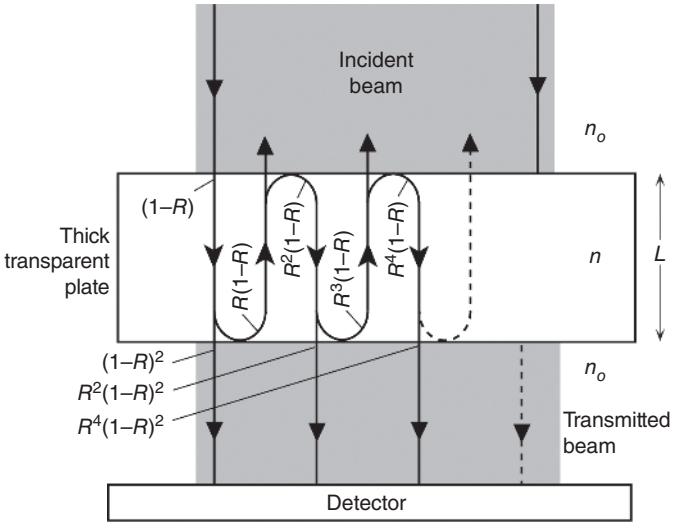

Figure 1.14 Transmitted and reflected light through a slab of material in which there is no interference.

resulting in a transmittance $T_{\text{plate}} = (1-R)^2 e^{-\alpha L} + R^2(1-R)^2 e^{-3\alpha L} + R^4(1-R)^2 e^{-5\alpha L} + \ldots$, so that the series sums to

$$T_{\text{plate}} = \frac{(1-R)^2 e^{-\alpha L}}{1 - R^2 e^{-2\alpha L}} \tag{1.46}$$

1.6 Optical Properties and Diffuse Reflection: Schuster–Kubelka–Munk Theory

The treatise in Section 1.4 on the analysis of the transmission spectrum $T(\lambda)$ assumes a smooth surface for the thin film and normal incidence. The propagating light wave through the film and its multiple reflections do not experience any scattering. The reflectance spectrum is simply $1 - T(\lambda)$. The situation is totally different if the film surface is rough or textured, and the bulk of the film exhibits scattering, which would be the case for particulate bulk material. The latter may be due to, for example, the polycrystallinity of the film, or the film may be a pressed powder layer or some composite with a mixture of two phases. Figure 1.15a shows a typical polycrystalline film sample with a rough surface whose optical properties are measured by *diffused reflection*. The nonspecular portion of light reflection is what constitutes the diffused reflection. There are many examples of diffused reflection from various forms of media, some of the most obvious being diffused reflection from rough surfaces, multiphase media, and multilayered translucent materials (e.g. paint coatings, paper, human skin, clothing, etc.). The instrumental setup is such that all light emitted over a wide solid angle is collected and the secularly reflected light is rejected—and hence the name. The experimental technique for implementing such measurements are well described in the literature (e.g. [119–127]), and there are various commercial instruments available from various vendors. The diffused reflectance spectrum is normally compared to a standard

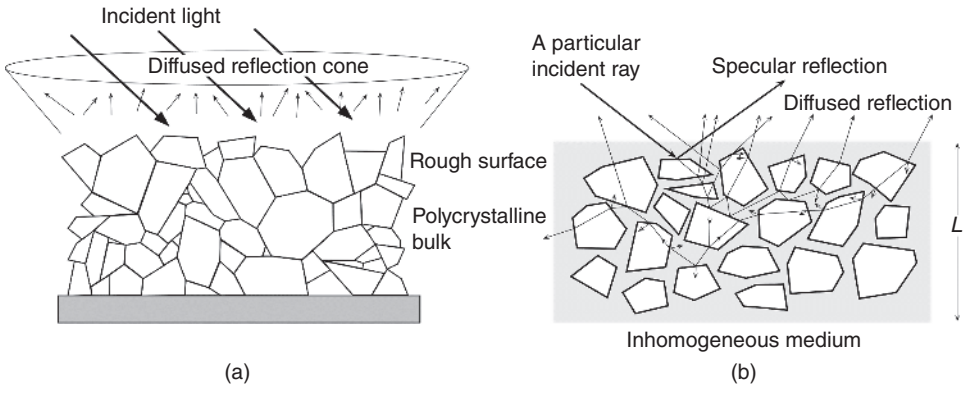

Figure 1.15 (a) Typical polycrystalline sample with a rough surface whose optical properties are measured by diffused reflection. (b) A simplified view of how diffused reflection builds up from scattering processes in the bulk.

by replacing the sample with a standard sample. Figure 1.15b shows a simplified view of how diffused reflection builds up from numerous refraction and reflection processes in the bulk so that the light is effectively scattered within the bulk. Although absorption is not shown, there would also be light extinction in the bulk.

The treatise of diffused reflection is mathematically a complicated problem due to the inhomogeneity of the medium. The basic question is, "*What are the suitable optical coefficients that can be used to describe the properties of the medium as related to diffused reflection*?" This issue has been reviewed and discussed extensively in the literature. The Kubelka–Munk (KM) formalism [128, 129] is a theory that relates the diffuse reflectance $R(\lambda)$ of a substance to multiple scattering and absorption within the substance. The treatise dates back to 1905 when Schuster quantitatively considered radiation traversing a foggy atmosphere [130], and hence the name *Schuster–Kubelka–Munk* (SKM) *theory*. The SKM formalism is widely used in various industrial [131–135] and biomedical applications [136, 137]. A recent practical review of diffuse reflectance with numerous references may be found in [126].

The KM theory addresses diffuse reflectance, and assigns two phenomenological coefficients labeled K and S to represent the absorption and scattering in the medium. K and S are used as coefficients that respectively indicate the amount of absorption and diffusion per unit thickness in the medium. K should not be confused with the extinction coefficient of the complex refractive index. It should be emphasized that K and S do not directly correspond to the intrinsic optical constants, that is, the absorption coefficient α, and the scattering coefficient s of the medium, although they are related. To describe the theory in simple terms, initially consider a medium such as a particulate layer (a layer of pressed powers), and assume that the sample is very thick (the sample thickness L is large, i.e. $KL \gg 1$), so that there is no reflection from or transmission through the rear surface of the sample. A *remission function* (also known as the KM or SKM function) $F(R)$ of diffuse reflectance R at a given wavelength is defined for the radiation absorption and scattering properties the medium of interest as

$$F \equiv F(R) = \frac{(1-R)^2}{R} = \frac{K}{S} \tag{1.47}$$

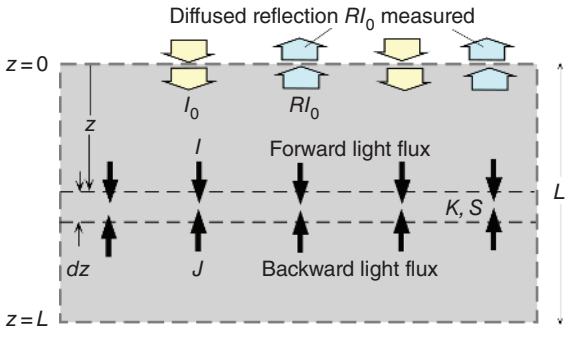

Figure 1.16 Medium with light absorption and scattering: K is the absorption and S is the scattering coefficient, that is, the fraction of light intensity absorbed or scattered, respectively, per unit distance. L is assumed to be large. I_0 is the intensity of light entering the medium.

where the function $F(R)$ represents a nearly steady-state intensity of diffuse reflectance R corresponding to an incident radiation at a wavelength λ. Figure 1.16 presents a two-flux diffuse-reflectance model of a semi-infinite diffusely reflecting medium in which the incident light I_0 toward the $+z$ direction is infinitesimally below the spectral refection surface medium [138]. The model considers the energy balance in a very thin layer (of thickness dz) in terms of diffuse intensities I and J, which are respectively along the forward ($+z$) and backward (−z) directions, as shown in Figure 1.16 [139], so that, over dz,

$$\frac{dI}{dz} = -(K + S)I + SJ \tag{1.48}$$

and

$$\frac{dJ}{dz} = (K + S)J - SI \tag{1.49}$$

Equations (1.48) and (1.49) can be applied as long as the particulate size is comparable to or smaller than λ. K and S have been proposed to be proportional (but not equal) to the usual optical absorption coefficient α and the scattering coefficient s, respectively, as discussed by Murphy [140, 141]; for example, $K = \varepsilon\alpha$, where ε is defined in such a way that it is the average path length traveled by diffuse light in crossing dz.

From Eqs. (1.48) and (1.49), it can be shown that

$$\frac{K}{S} = \frac{(1 - R)^2}{2R} \tag{1.50}$$

For an infinitely thick medium, $R = J/I$ and Eq. (1.50) provides K/S.

Equation (1.50) provides a useful way of using the diffusive reflectance spectrum to extract the absorption spectrum. The rearrangement of Eq. (1.50) gives an explicit expression for R as

$$R = (1 + K/S) - [(1 + K/S)^2 - 1]^{1/2} \tag{1.51}$$

The remission function $F(R)$ and K for a weakly absorbing powdered medium of thickness L may be written in terms of fundamental optical parameters n and α through [139],

$$F = \frac{2n^2\alpha L}{3} \tag{1.52}$$

and

$$K = \frac{2n^2\alpha}{3} \tag{1.53}$$

The particles are assumed to be spherical with rough surfaces, and the particle dimeter is larger than the wavelength. Notice that K is not the same as α. Although the relatively simple equations in the preceding text are attractive to experimentalists, a more rigorous treatise shows that the relationships between K and S and the material absorption and scattering coefficients α and s involve the ratio μ of the total optical path length of a photon from its entry point (from one scattering process to the next) to its effective displacement from the entry point [142]. The problem immediately becomes analytically intractable without simplifying assumptions. In this model, K is proportional to α through the ratio μ.

The Tauc law, which has been widely used for determining the bandgap of various semiconductors, has also been adapted in recent years (e.g. [143–148]) for the diffuse reflectance spectrum in terms of a transformed KM function $h\nu F(R)$, that is,

$$\left[h\nu F(R)\right]^p = B(h\nu - E_g) \tag{1.54}$$

where B is a constant (independent of photon energy) and p is an index, typically 1/3 to 2, that depends on the nature of the transition and the states that are involved. (The Tauc law is discussed in Chapter 3 in connection with amorphous semiconductors, but, in the form in Eq. (1.54), it represents a general description of absorption for photon energies just above the bandgap energy.) The rationale for Equation (1.54) is based F being proportional to α. Figure 1.17 shows a diffuse reflectance spectra within the UV and visible region (400 nm $< \lambda <$ 860 nm) for a composite film of methylammonium iodide (CH_3NH_3I) and lead iodide (PbI_2) in a 1 : 4 weight ratio. The Tauc plot is also shown and points to a bandgap E_g of 1.49 eV. Equation (1.54) has had success for estimating E_g for powder-form nanomaterials yielding experimentally supported values as reported in [150].

Alternative descriptions for characterizing the optical properties of coating materials have also been available for Eq. (1.51) in the literature. For example, the diffuse reflectance from a layer of finite thickness L on a substrate having a reflectance R_g is

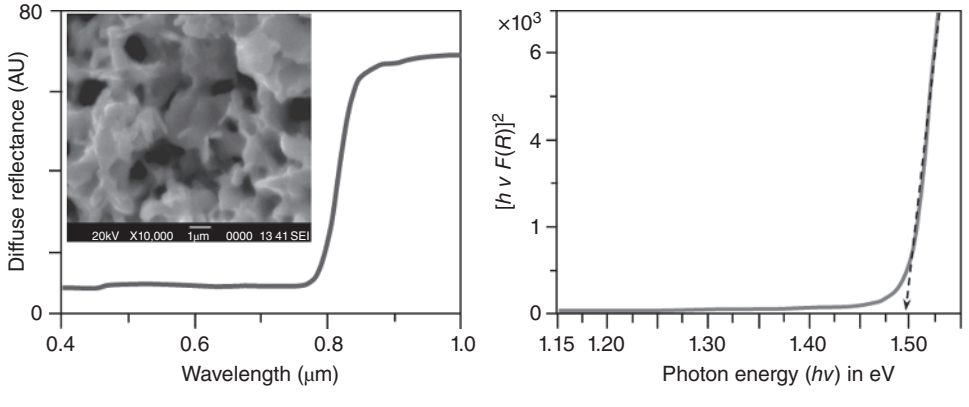

Figure 1.17 UV-visible diffuse reflectance spectra (left) and the Tauc-like plot (right) with $p = 2$ of a Perovskite film (550 nm thick) containing methylammonium iodide (CH_3NH_3I) and lead iodide (PbI_2) in weight ratios of 1 : 4. The inset shows an SEM image of the microstructure, which consists of a random distribution of pores (voids) (AU is "arbitrary units"). The data were extracted, reanalyzed, and replotted from [149].

given as [140]:

$$R = \frac{1 - R_g[a - b\coth(bSL)]}{a + b\coth(bSL) - R_g} \tag{1.55}$$

in which $a = 1 + K/S$ and $b = [a^2 - 1]^{1/2}$. The assumptions in Eq. (1.55) are that the light arrives from a medium that has the same refractive index as the layer, and that scattering is isotropic within the medium.

In the case of a homogenous slab that has a thickness L, the diffuse reflectance R at a given wavelength can be written as

$$R = \frac{(1 - \beta^2)\sinh(\kappa L)}{(1 + \beta^2)\sinh(\kappa L) + 2\beta\cosh(\kappa L)} \tag{1.56}$$

where $\beta = [K/(K + 2S)]^{1/2}$and $\kappa = [K(K + 2S)]^{1/2}$. Fitting this equation to the observed reflectance would yield β and κ, and hence K and S. However, Eq. (1.51), in many cases, has been found to be adequate for the interpretation of the spectra from high-emissive coatings with no significant effect of its covering power color building in visible and near-infrared spectral range [151]. The usefulness of the KM theory is due to the fact that the scattering and the absorption constants K and S tend to scale linearly with the concentration of colorants or pigments, and the overall contributions of colorants, inks, and pigments can be found by applying an additive rule, that is, adding the individual KL together for absorption and individual SL for scattering.

The interpretation of diffuse reflectance spectra $R(\lambda)$ and the extraction of meaningful optical coefficients continue to be an active research area. There have been several important reviews and useful criticisms of the simplified KM approach described above, which should be considered [141, 142, 152–154].

1.7 Conclusions

This chapter has provided a semiquantitative explanation and discussion of the complex refractive index $n^* = n + iK$; the relationship between the real n and imaginary part K through the Kramers–Kronig relationships; various common dispersion (n vs. λ) relationships such as the Cauchy, Sellmeier, Wemple–DiDomenico dispersion relations; and the determination of the optical constants of a material in thin film form using the popular Swanepoel technique. The latter technique is based on the interference of waves in the thin film, and uses the maxima and minima in the transmittance spectrum to extract the dispersion relation for n and K. The transmittance of light through a thick semitransparent plate is also considered. The KM formulism is described in a simplified way to interpret diffuse reflection from inhomogeneous coating and/or rough surfaces. Examples are given to highlight the concepts and provide applications. The optical constants of various selected materials have been also provided in tables to illustrate typical values and enable comparisons.

Acknowledgments

The authors are most grateful to Cyril Koughia for his helpful comments and assistance during the preparation of the first edition of this chapter.

References

1 Greenaway, D.L. and Harbeke, G. (1968). *Optical Properties and Band Structure of Semiconductors*. Oxford: Pergamon Press.
2 Wolfe, W.L. (1978). *The Handbook of Optics* (eds. W.G. Driscoll and W. Vaughan). New York: McGraw-Hill.
3 Klocek, P. (ed.) (1991). *Handbook of Infrared Optical Materials*. New York: Marcel Dekker.
4 Palik, E.D. (ed.) (1985). *Handbook of Optical Constants of Solids*. San Diego: Academic Press (now Elsevier).
5 Palik, E.D. (ed.) (1991). *Handbook of Optical Constants of Solids II*. San Diego: Academic Press (now Elsevier).
6 Ward, L. (1994). *The Optical Constants of Bulk Materials and Films*. Bristol: Institute of Physics Publishing (reprint 1998).
7 Efimov, A.M. (1995). *Optical Constants of Inorganic Glasses*. Boca Raton: CRC Press.
8 Palik, E.D. and Ghosh, G.K. (eds.) (1997). *Handbook of Optical Constants of Solids*, vol. 1-5. San Diego: Academic Press (now Elsevier).
9 Nikogosyan, D. (1997). *Properties of Optical and Laser-Related Materials: A Handbook*. New York: Wiley.
10 Weaver, J.H. and Frederickse, H.P.R. (1999). *CRC Handbook of Chemistry and Physics* (ed. D.R. Lide). Boca Raton: CRC Press, Ch 12.
11 Adachi, S. (1992). *Physical Properties of III-V Semiconductor Compounds*. New York: Wiley.
12 Adachi, S. (1999). *Optical Constants in Crystalline and Amorphous Semiconductors: Numerical Data and Graphical Information*. Boston: Kluwer Academic Publishers.
13 Adachi, S. (2005). *Properties of Group-IV, III-V and II-VI Semiconductors*. Chichester: Wiley.
14 Madelung, O. (2004). *Semiconductors: Data Handbook*, 3e. New York: Springer-Verlag.
15 Bass, M. (ed.) (2010). *Handbook of Optics*, 3e, vol. 2. New York: McGraw-Hill, Chapters 35 (Properties of Materials), 36 (Optical Properties of Semiconductors).
16 Nalwa, H.S. (ed.) (2001). *Handbook of Advanced Electronic and Photonic Materials and Devices*, vol. 1–10. San Diego: Academic Press (now Elsevier).
17 Weber, M.J. (2003). *Handbook of Optical Materials*. Boca Raton: CRC Press.
18 Martienssen, W. and Walimont, H. (eds.) (2005). *Springer Handbook of Condensed Matter and Materials Data*. Heidelberg: Springer, various sections.
19 Kasap, S.O. and Capper, P. (eds.) (2017). *Springer Handbook of Electronic and Photonic Materials*, 2e. Heidelberg: Springer Chapter 3.
20 Novak, M. (2013). Optical properties of semiconductors, Ch. 7. In: *Silicon Based Thin Films* (ed. R. Murri), 177–242. Bentham Books.
21 Tanner, D.B. (2019). *Optical Effects in Solids, University of Florida*. Cambridge: Cambridge University Press.
22 Jimenez, J. and Tomm, J.W. (2016). *Spectroscopic Analysis of Optoelectronic Semiconductors*. Switzerland: Springer International Publishing.
23 Stenzel, O. (2014). *Optical Coatings*. Heidelberg: Springer-Verlag.
24 Fox, M. (2010). *Optical Properties of Solids*, 2e. Oxford: Oxford University Press.

25 Simmons, J.H. and Potter, K.S. (2000). *Optical Materials*. San Diego: Academic Press (now Elsevier).
26 Toyozawa, Y. (2003). *Optical Processes in Solids*. Cambridge: Cambridge University Press.
27 Wooten, F. (1972). *Optical Properties of Solids*. New York: Academic Press (now Elsevier).
28 Abeles, F. (1972). *Optical Properties of Solids*. Amsterdam: North Holland (now Elsevier).
29 Collins, R.W. (2004). Ellipsometery. In: *The Optics Encyclopedia*, vol. 1 (eds. T.G. Brown, K. Creath, H. Kogelnik, et al.), 609–670. Weinheim: Wiley-VCH.
30 Kasap, S.O. (2017). *Principles of Electronic Materials and Devices*, 4e. New York: McGraw-Hill Higher Education Chs 7 and 9.
31 Philipp, H.R. and Taft, E.A. (1960). *Phys. Rev.* 120: 37.
32 Aspnes, D.E. and Studna, A.A. (1983). *Phys. Rev.* B27: 985.
33 Kronig, R. (1926). *J. Opt. Soc. Amer.* 12: 547.
34 H.A. Kramers (1927). *Estratto Dagli Atti del Congresso Internazionale de Fisici*, **2**, 545.
35 Nussenzveig, H.M. (1972). Ch. In: *Causality and Dispersion Relations1*. New York: Academic Press, Inc.
36 Suzuki, N. and Adachi, S. (1994). *Jpn. J. Appl. Phys.* 33: 193.
37 Nitsche, R. and Fritz, T. (2004). *Phys. Rev. B* 70: 195432.
38 Bhattacharyya, D. and Biswas, A. (2005). *J. Appl. Phys.* 97: 053501.
39 Yim, C., O'Brien, M., McEvoy, N. et al. (2014). *Appl. Phys. Lett.* 104: 103114.
40 Choi, S.G., Kang, J., Li, J. et al. (2015). *Appl. Phys. Lett.* 106: 043901.
41 Jellison, G.E. and Modine, F.A. (1996). *Appl. Phys. Lett.* 69: 371.
42 Forouhi, A.R. and Bloomer, I. (1988). *Phys. Rev. B* 38: 1865.
43 Smith, D.Y. and Shiles, E. (1978). *Phys. Rev. B* 17: 4689.
44 https://refractiveindex.info (Accessed, 12 August 2018)
45 Cauchy, A.L. (1830). *Bull. Sci. Math.* 14: 6.
46 Cauchy, A.L. (1836). *Memoire sur la Dispersion de la Lumiere*. Prague: Calve.
47 Smith, D.Y., Inokuti, M., and Karstens, W. (2001). *J. Phys. Cond. Matt.* 13: 3883.
48 Sellmeier, W. (1871). *Ann. der Phys.* 143: S272.
49 Tatian, B. (1984). *Appl. Opt.* 23: 4477.
50 Fleming, J.W. (1984). *Appl. Opt.* 23: 4486.
51 Wolf, K.L. and Herzfeld, K.F. (1928). *Handbooch der Physik*, vol. 20, Ch. 10 (eds. H. Geiger and K. Scheel). Berlin: Springer Verlag.
52 Herzberger, M. (1959). *Opt. Acta* 6: 197.
53 Bachs, H. and Neuroth, N. (eds.) (1995). *Schott Series on Glass and Glass Ceramics*. Heidelberg: Springer.
54 Kreidl, N.J. and Uhlmann, D.R. (eds.) (1991). *Optical Properties of Glass*. The American Ceramic Society.
55 Hawkins, G. and Hunneman, R. (2004). *Infrared Phys. Technol.* 45: 69.
56 Forouhi, A.R. and Bloomer, I. (1986). *Phys. Rev. B* 34: 7018.
57 Chen, Y.F., Kwei, C.M., and Tung, C.J. (1993). *Phys. Rev. B* 48: 4373.
58 Afromowitz, M.A. (1974). *Solid State Commun.* 15: 59.
59 Adachi, S. (1982). *J. Appl. Phys.* 53: 5863.
60 Adachi, S. (1988). *Phys. Rev. B* 38: 12345.

61 Adachi, S. (1987). *Phys. Rev. B* 35: 123161.
62 Adachi, S. (1991). *Phys. Rev. B* 43: 123161.
63 Adachi, S., Mori, H., and Ozaki, S. (2002). *Phys. Rev. B* 66: 153201.
64 Campi, D. and Papuzza, C. (1985). *J. Appl. Phys.* 57: 1305.
65 Rakic, A.D. and Majewski, M.L. (1996). *J. Appl. Phys.* 80: 5909.
66 Erman, M., Theeten, J.B., Chambon, P. et al. (1984). *J. Appl. Phys.* 56: 2664.
67 Terry, F.L. (1991). *J. Appl. Phys.* 70: 409.
68 Johs, B., Herzinger, C.M., Dinan, J.H. et al. (1988). *Thin Solid Films* 314: 137.
69 Kim, T.J., Ghong, T.H., Kim, Y.D. et al. (2003). *Phys. Rev. B* 68: 115323.
70 Hwang, S.Y., Kim, T.J., Byun, J.S. et al. (2013). *Thin Solid Films* 547: 276.
71 Moss, T.S. (1950). *Proc. Phys. Soc. B* 63: 167.
72 Moss, T.S. (1985). *Phys. Status Solidi B* 131: 415.
73 Hervé, P.J.L. and Vandamme, L.K.J. (1996). *J. Appl. Phys.* 77: 5476.
74 Kumar, V. and Singh, J.K. (2010). *Ind. J. Pure Appl. Phys.* 48: 571–574.
75 Moss, T.S. (1952). *Photoconductivity in the Elements*. New York: Academic Press.
76 Ravindra, N.M., Auchuluk, S., and Srivastava, V.K. (1979). *Phys. Stat. Solidi B* 93: K155.
77 Finkenrath, H. (1988). *Infrared Phys.* 28: 327.
78 Reddy, R.R., Nazeer Ahammed, Y., Rama Gopal, K., and Raghuram, D.V. (1998). *Opt. Mater.* 10: 95.
79 Duffy, J.A. (2001). *Phys. Chem. Glass* 42: 151.
80 Reddy, R.R. and Nazeer Ahammed, Y. (1995). *Cryst. Res. Technol.* 30: 263.
81 Reddy, R.R. and Nazeer Ahammed, Y. (1995). *Infrared Phys. Technol.* 36: 825.
82 Dale, D. and Gladstone, F. (1858). *Philos. Trans.* 148: 887.
83 Dale, D. and Gladstone, f. (1863). *Philos. Trans.* 153: 317.
84 Ritland, H.N. (1955). *J. Am. Ceram. Soc.* 38: 86.
85 SCHOTT (2016). Technical Information TIE29, Refractive Index and Dispersion (available online at http:// www.schott.com; accessed 12 August 2018
86 Hoffmann, H., Jochs, W., and Westenberger, G. (1992). *SPIE Proc.* 1780: 303.
87 Ghosh, G., Endo, M., and Iwasaki, T. (1994). *J. Light Wave Technol.* 12: 1338.
88 Ghosh, G. (1997). *Appl. Opt.* 36: 1540.
89 Ghosh, G. (1998). *Phys. Rev. B* 14: 8178.
90 Englert, M., Hartmann, P., and Reichel, S. (2014); https://doi). *SPIE Proc.* 9131: 91310H. doi: 10.1117/12.2052706.
91 Wemple, S.H. and DiDomenico, M. Jr., (1971). *Phys. Rev. B* 3: 1338.
92 Wemple, S.H. (1973). *Phys. Rev. B* 7: 3767.
93 Henry, C.H., Johnson, L.F., Logan, R.A., and Clarke, D.P. (1985). *IEEE J. Quantum Electron.* QE21: 1881.
94 Wemple, S.H. (1977). *J. Chem. Phys.* 67: 2151.
95 Kasap, S.O. (2013). *Optoelectronics and Photonics: Principles and Practices*, 2e. Upper Saddle River, NJ: Pearson Education Ch 1.
96 Heavens, O.S. (1965). *Optical Properties of Thin Solid Films*. New York: Dover Publications (Reprint 1991).
97 Poelman, D. and Smet, P.F. (2003). *J. Phys. D. Appl. Phys.* 36: 1850. and references therein.
98 Swanepoel, R. (1983). *J. Phys. E Sci. Instrum.* 16: 1214.
99 Manifacier, J.C., Gasiot, J., and Fillard, J.P. (1976). *J. Phys. E Sci. Instrum.* 9: 1002.

100 Hall, J.F. and Ferguson, W.F.C. (1955). *J. Opt. Soci. Am.* 145: 714.
101 Swanepoel, R. (1984). *J. Phys. E Sci. Instrum.* 17: 896.
102 Marquez, E., Ramirez-Malo, J.B., Villares, P. et al. (1995). *Thin Solid Films* 254: 83.
103 Caricato, A.P., Fazzi, A., and Leggieri, G. (2005). *Appl.Surf. Sci.* 248: 440. and references therein.
104 Chambouleyron, I., Ventura, S.D., Birgin, E.G., and Martínez, J.M. (2002). *J. Appl. Phys.* 92: 3093. and references therein.
105 Ayadi, K. and Haddaoui, N. (2000). *J. Mater. Sci. Mater. Electron.* 11: 163.
106 Jin, Y., Song, B., Jia, Z. et al. (2017). *Opt. Exp.* 25: 440.
107 Marquez, E., Ramirez-Malo, J., Villares, P. et al. (1992). *J. Phys. D* 25: 535.
108 Márquez, E., González-Leal, J.M., Prieto-Alcón, R. et al. (1998). *Appl. Phys. A Mater. Sci. Process.* 67: 371.
109 Gonzalez-Leal, J.M., Ledesma, A., Bernal-Oliva, A.M. et al. (1999). *Mater. Lett.* 39: 232.
110 Marquez, E., Bernal-Oliva, A.M., GonzaÂlez-Leal, J.M. et al. (1999). *Mater. Chem. Phys.* 60: 231.
111 Moharram, A.H., Othman, A.A., and Osman, M.A. (2002). *Appl. Surf. Sci.* 200: 143.
112 Bakr, N.A., El-Hadidy, H., Hammam, M., and Migahed, M.D. (2003). *Thin Solids Films* 424: 296.
113 Gonzalez-Leal, J.M., Prieto-Alcon, R., Angel, J.A., and Marquez, E. (2003). *J. Non-Crystalline Solids* 315: 134.
114 El-Sayed, S.M. and Amin, G.A.M. (2005). *ND&E Int.* 38: 113.
115 Tigau, N., Ciupina, V., and Prodan, G. (2005). *J. Crystal Growth* 277: 529.
116 Fayek, S.A. and El-Sayed, S.M. (2006). *ND&E Int.* 39: 39.
117 Sanchez-Gonzalez, J., Dıaz-Parralejo, A., Ortiz, A.L., and Guiberteau, F. (2006). *Appl. Surf. Sci.* 252: 6013–6017.
118 Fang, Y., Jayasuriya, D., Furniss, D. et al. (2017). *Opt. Quant. Electron.* 49: 237.
119 Companion, A.L. Theory and applications of diffuse reflectance spectroscopy. In: *Developments in Applied Spectroscopy*, vol. 4 (ed. E.N. Davis), 221–233. Boston, MA: Springer.
120 Hecht, W.W.M. and Wendlandt, H.G. (1966). *Reflectance spectroscopy (Chemical analysis)*, 91–209. Wiley Interscience Publishers.
121 Kortüm, G. (1969). *Reflectance Specroscopy: Principles, Methods, Applications*. New York: Springer Verlag Chs 5 and 6.
122 Fuller, M.P. and Griffiths, P.R. (1978). *Analy. Chem.* 50: 1906.
123 Delgass, W.N., Haller, G.L., Kellerman, R., and Lunsford, J.H. (1979). *Spectroscopy in Heterogenous Catalysis*. New York: Academic Press Ch 4.
124 Blitz, J.P. Ch 5: Diffuse reflectance spectroscopy. In: *Modern Techniques in Applied Molecular Spectroscopy* (ed. F.M. Mirabella), 1998. New York: Wiley.
125 Weckhuysen, B.M. and Schoonheydt, A. (1999). *Catal. Today* 49: 441–451.
126 Jentoft, F.C. (2009). *Adv. Catal.* 52: 129. and references therein.
127 Monsef Khoshhesab, Z. (2012). *Infrared Spectroscopy - Materials Science, Engineering and Technology* (ed. T. Theophile). Rijeka, Croatia: InTech (ISBN: 978-953-51-0537-4); Ch 11 "Reflectance IR Spectroscopy".
128 Kubelka, P. and Munk, F. (1931). *Z. Tech. Phys. (Leipzig)* 12: 593.
129 Kubelka, P. (1948). *J Opt Soc* 38: 448.
130 Schuster, A. (1905). *Astrophys. J.* 21: 1.

131 Q. Zeng, M. Cao, X. Feng, F. Liang, X. Chen and W. Sheng (1983). A study of spectral reflection characteristics for snow, ice and water in the north of China, *Hydrological Applications of Remote Sensing and Remote Data Transmission* (Proceedings of the Hamburg Symposium). IAHS Publ. no. 145
132 Dzimbeg-Malcic, V., Barbaric-Mikocevic, Z., and Itric, K. (2011). *Teh. Vjesn.* 18: 117.
133 Dingemans, L.M., Papadakis, V.M., Liu, P. et al. (2017). *J. Eur. Opt. Soc. Rapid Publ.* 13 Article Number: 40. https://doi.org/10.1186/s41476-017-0068-2.
134 Rogers, G. (2016). *Color. Res. Appl.* 41: 580.
135 Džimbeg-Malčić, V., Barbarić-Mikočević, Ž., and Itrić, K. (2011). *Technical Gazette (Croatia)* 18: 117.
136 Gorpas, D., Alexandratou, E., Politopoulos, K., and Yova, D. (2005). Diagnostic algorithms based on Kubelka-Munk theory to discriminate healthy and Atheromatous aorta in animal model. *Proc. SPIE* 5268: 235.
137 Reuter, T., Karl, S., Hoffmann, M.B., and Dietzek, B. (2013). *Biomed. Eng.* 58 (Suppl. 1) https://doi.org/10.1515/bmt-2013-435.
138 Myrick, M.L., Simcock, M.N., Baranowski, M. et al. (2011). *Appl. Spectrosc. Rev.* 46: 140.
139 Simmons, E.L. (1972). *Opt. Acta* 19: 845–851.
140 Murphy, A.B. (2006). *J. Phys. D. Appl. Phys.* 39: 3571.
141 Murphy, A.B. (2007). *Appl. Opt.* 46: 3133.
142 Yang, L. and Kruse, B. (2004). *J. Opt. Soc. Am.* 21: 1933.
143 Escobedo Morales, A., Sánchez Mora, E., and Pal, U. (2007). *Rev. Mex. Fis.* 53: 18.
144 Nowak, M., Kauch, B., and Szperlic, P. (2009). *Rev. Sci. Intrum.* 80: 046107.
145 Yakuphanoglu, F. (2010). *J. Alloys Compd.* 507: 184.
146 Lopez, R. and Gómez, L.R. (2012). *J. Sol-Gel Sci. Technol.* 61: 1.
147 Caglar, Y., Görgün, K., Ilican, S. et al. (2016). *Appl. Phys. A* 122 (733).
148 Nam-GyuPark (2015). *Mater. Today* 18: 65.
149 Mahapatra, S.K., Saykar, N., Banerjee, I. et al. (2018). *J. Mater. Sci. Mater. Electron.* https://doi.org/10.1007/s10854-018-9992-1.
150 Ahsan, R., Khan, M.Z.R., and Basith, M.A. (2017). *J. Nanophoton.* 11: 046016.
151 He, Y., Zhang, X., and Zhang, Y.J. (2016). *Wuhan Univ. Technol. Mat. Sci. Edit.* 31: 100.
152 Nobbs, J.H. (1985). *Rev. Prog. Coloration* 15: 66.
153 R.A. de la Osa, A. Fernandez, Y. Gutierrez, D. Ortiz, F. Gonzalez, F. Moreno, J.M. Saiz (2017). The extended Kubelka-Munk theory and its application to colloidal systems. Third International Conference on Applications of Optics and Photonics**,** Proceedings of SPIE**, 10453,** 104531F 8 pp. DOI: 10.1117/12.2272115
154 Wang, J., Xu, C., Nilsson, A.M. et al. (2019). *Adv. Optical Mater* 7: 1801315.